Archives of Computational Methods in Engineering
https://doi.org/10.1007/s11831-022-09811-x

SURVEY ARTICLE

A Comprehensive Survey with Quantitative Comparison of Image Analysis Methods for Microorganism Biovolume Measurements

Jiawei Zhang[1] · Chen Li[1] · Md Mamunur Rahaman[1,6] · Yudong Yao[2] · Pingli Ma[1] · Jinghua Zhang[1,5] · Xin Zhao[3] · Tao Jiang[4] · Marcin Grzegorzek[5]

Received: 5 May 2021 / Accepted: 22 August 2022
© The Author(s) under exclusive licence to International Center for Numerical Methods in Engineering (CIMNE) 2022

Abstract
With the acceleration of urbanization and living standards, microorganisms play an increasingly important role in industrial production, bio-technique, and food safety testing. Microorganism biovolume measurements are one of the essential parts of microbial analysis. However, traditional manual measurement methods are time-consuming and challenging to measure the characteristics precisely. With the development of digital image processing techniques, the characteristics of the microbial population can be detected and quantified. The applications of the microorganism biovolume measurement method have developed since the 1980s. More than 62 articles are reviewed in this study, and the articles are grouped by digital image analysis methods with time. This study has high research significance and application value, which can be referred to as microbial researchers to comprehensively understand microorganism biovolume measurements using digital image analysis methods and potential applications.

1 Introduction

1.1 Basic Knowledge of Microorganisms

Microorganisms are kinds of tiny organisms that are distributed all around the world. They exist in people's daily life but cannot be discovered by naked eyes. Various microscopes are designed to observe the microorganism precisely [1]. Microorganisms are classified into a large number of types based on different classification standards. Generally, microorganisms consist of bacteria, viruses, fungi, and algae.

Bacteria are the most common unicellular organisms globally, which have a tiny size and simple biological structure. They lack nuclei, cytoskeletons, and membranous, and most of them are decomposers that can decompose dead organisms into simple inorganic substances and release energy, such as the works of *Bacillus subtilis*. Viruses are kinds of microorganisms with a simple structure that can infect other organisms. It contains nucleic acid, such as ribonucleic acid (RNA) and deoxyribonucleic acid (DNA). The healthy cells are parasitized and produce the nutrition for virus propagation [2]. Viruses are harmful to human and agricultural production. For instance, the severe acute respiratory syndrome coronavirus 2 (SARS-CoV-2) has caused significant loss of life and property all over the world [3, 4]. Fungi are kinds of eukaryotic, sporogenic, chloroplast-free eukaryotes that contain molds, yeasts and other mushrooms known. The spores are produced by sexual and asexual propagation. Fungi play an essential role in agriculture and industrial production [5]. Algae are a group of eukaryotes of the Protista. Most of them are aquatic, without vascular bundles, and can carry out photosynthesis. Some algae are single-celled dinoflagellates, while others aggregate into colonies. Algae play essential roles in food production, such as *Undaria pinnatifida* and *Laminaria japonica*, which can

✉ Chen Li
lichen201096@hotmail.com

1 Microscopic Image and Medical Image Analysis Group, College of Medicine and Biological Information Engineering, Northeastern University, Shenyang 110169, China

2 Department of Electrical and Computer Engineering, Stevens Institute of Technology, Hoboken, NJ 07030, USA

3 School of Resources and Civil Engineering, Northeastern University, Shenyang 110004, China

4 School of Intelligent Medicine, Chengdu University of Traditional Chinese Medicine, Chengdu 610225, China

5 Institute of Medical Informatics, University of Luebeck, Luebeck 23538, Germany

6 School of Computer Science and Engineering, University of New South Wales, Sydney, NSW 2052, Australia

Published online: 06 September 2022

be used for medical purposes, like preventing and treating goitre [6].

Microorganisms are in various forms. Some are corrupt, which can cause food decomposition and adverse changes to organizational structure, but some are beneficial. For example, healthy people have a large number of bacteria in the stomach. The normal flora contains hundreds of species of bacteria. These bacteria are mutually dependent and mutualistic in the gut environment, and the disorder of bacteria can lead to diarrhea. However, some microorganisms are harmful to human health and society production. Acquired immune deficiency syndrome (AIDS) is a dangerous infectious disease caused by the human immunodeficiency virus (HIV), which can attack the body's immune system. The CD4T lymphocytes system, which is an essential part of the human immune system, is attacked violently, the cells are destroyed in large numbers, and causes the loss of immune function in the human body; SARS-CoV-2 broke out in 2019 [7, 8], and it continues to be widely spread. More than 120,000,000 people have been infected globally till March 17th, 2021, which has caused huge economic and productivity losses [9].

Because of microorganisms' vital role globally, related microbial research is continuously developing. Microorganism quantification is one of the most important parts of microbial research. It is widely used in food and water safety test, biomedical test and environmental surveillance [10]. There are two main methods for microorganism biovolume measurement one is manual measurement, and the other is computer image analysis-based measurement [11]. Manual measurement mainly includes the biovolume and dry cell weight (DCW) measurement methods. The biovolume measurement method reflects the growth state of microorganisms by measuring the volume of mycelia contained in a certain volume of culture medium. It has the advantage of being fast and straightforward, but the deviation is relatively large. The culture medium usually contains non-bacterial solid substances that can cause measurement errors. Moreover, it does not apply to the medium for mash fermentation. DCW method is applied by collecting a unit volume of microbial culture solution through centrifugation and repeatedly washing the microorganisms with water. After frequent pressure or vacuum drying, the total biomass of the culture can be calculated by accurate weighing. In an environment with high target microorganism content and less non-bacterial particle impurities, it is more accurate, but it is cumbersome and time-consuming, which is not convenient for online analysis. The advantages of manual measurements are that when the sample is clear with fewer impurities, the measurement speed is rapid, resulting in higher accuracy. Nevertheless, when the sample is turbid, the impurities cannot be excluded completely, and the measurement system cannot distinguish impurity debris from target microorganisms, so the target microorganisms cannot be measured accurately. Moreover, the measurement results are subjective, and the staff's workload is as heavy and frustrating, probably leading to deviation due to fatigue [12].

An automatic computer-aided image analysis system can significantly reduce the workload and enhance accuracy [13, 14]. The different microorganism measurement methods are applied because of the different microorganism species and microscopic imaging methods.

Some images with larger magnification and more scattered colonies can be measured by image analysis. In Fig. 1, an image of a *Candida* yeast cell is shown. It has shown a clear boundary that can be separated. After that, the measurement of parameters such as area and perimeter can be obtained readily, and the number of objects can be counted precisely. The corresponding survey of microorganism counting approaches can be found in our latest work [15] for detail.

The approaches to microorganism biovolume measurement are different from those of microorganism counting. Biovolumes can be measured from each species or genus's geometric shape and size, including categorizing some genera by morphology. However, in some cases, the biovolume cannot be measured by using relationships between microorganism counts and the biovolume of each identified microorganism species or genus [17]. Some images are blurred with smaller magnification and not clear enough for separation. For example, algae and fungi are entangled with each other that cannot be separated. Biovolume measurement can be

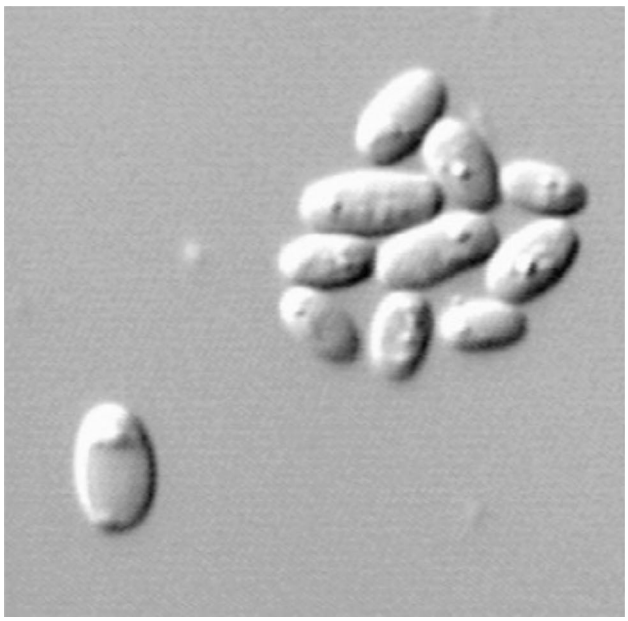

Fig. 1 The image of yeast cells, which shown the clear boundary between them (in [16] Fig. 3a)

used for quantification for this purpose. In Fig. 2, an image of fungal hyphae with complex distribution is illustrated.

In Fig. 3, the mycelia image is shown. The classical measurement method of mycelial morphology relies on inaccurate and time-consuming manual measurements from images because of the random distribution of entangled mycelial. Moreover, the method cannot measure the hyphal branches individually.

1.2 Motivation of This Review

Digital Image Processing (DIP) is applied for image denoising, image enhancement, image segmentation and feature extraction by using a computer. DIP is firstly used in the 1950s, the computer is designed and can be applied to process graphics information to improve the image resolution [20]. DIP has been widely used in many fields. Agricultural and forestry departments can detect pesticides in vegetables, identify the rice varieties, design various piking robots and monitor the management of diseases and insect pests [21]. The water conservancy department can prevent the disaster of water in advance through remote sensing image analysis [22]. Image segmentation technology, image description method and pattern recognition technology are used to identify and detect fire disaster [23]. The traffic controlling department can use DIP to monitor the road condition, recognize license plate number, and violate detection [24]. Medical departments can use amounts of DIP technology to automatically classify and segment various diseases [25–29]. The professional equipment is necessary for microbial researches to achieve the better precision. However, the use of DIP can reduce the equipment costs [30]. Meanwhile, DIP has been applied in the field of microorganism biovolume measurement widely. The trend of development is shown in Fig. 4.

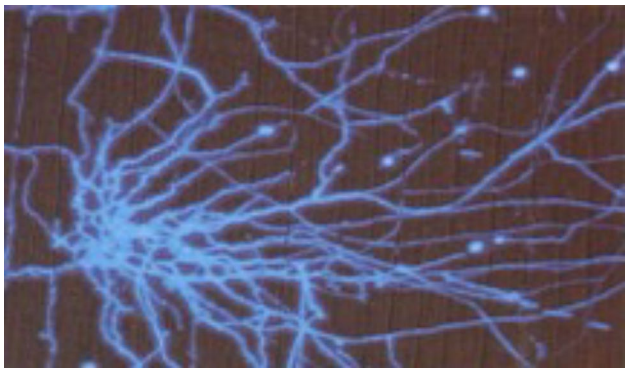

Fig. 2 The image of fungi hyphae in soil that are stained for observing (in [18] Fig. 2)

It can be seen that the use of DIP in the field of microorganism biovolume measurement maintains an upward trend. Since 1980s, DIP has been applied to microorganism biovolume measurement. From 1980 to 1995, the development are relatively slow. The developments of microorganism biovolume measurement are relatively rapid from 1995 to 2010. However, after 2010, the biovolume measurement related research entered the platform period. According to the content of the papers, summed up two possible reasons for the development situation. At first, due to the development of the algorithm, especially the development of deep learning, more accurate image segmentation can be achieved. For example, the segmentation of adherent colonies can lead to more accurate microorganism counting. Secondly, it is very difficult to obtain the three-dimensional data only from the image. Image analysis can obtain the surface areas of microorganisms, but cannot accurately calculate their volume. Accurate quantification will be a challenging task without a more accurate instrument.

Since microorganism counting and biovolume measurement suit different cases: In our previous work [15], there

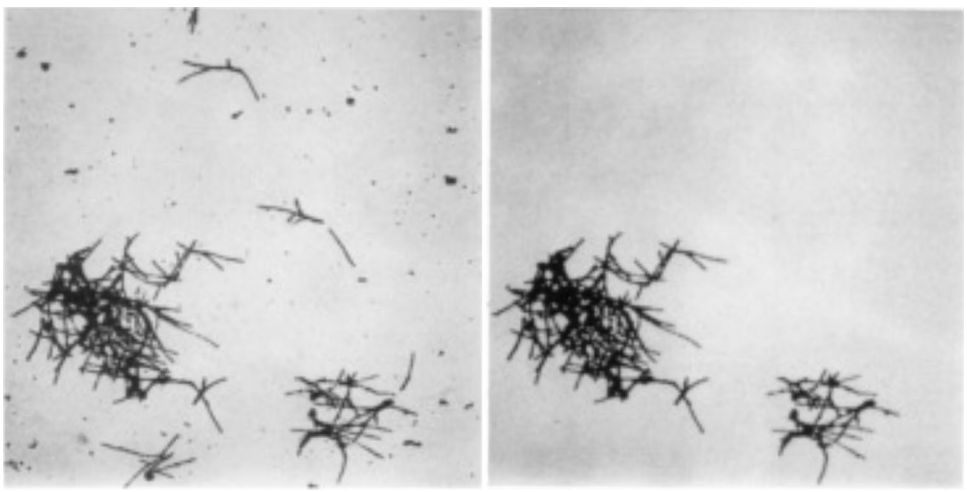

Fig. 3 The mycelia images obtained through the program (in [19] Fig. 1)

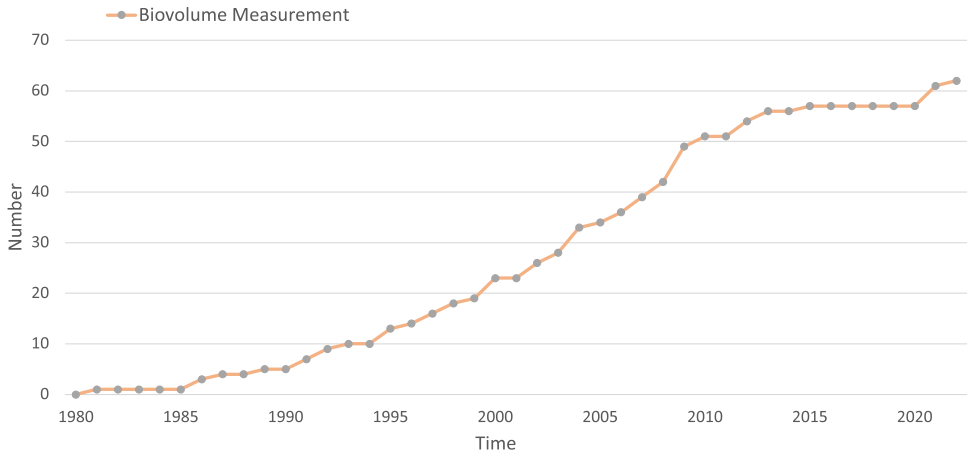

Fig. 4 The total number of related works on microorganism biovolume measurement approaches

were more than 132 papers for microorganism counting; in this study, there are 58 papers for biovolume measurement. Among all these papers, only four papers are overlapping [31–34], both for microorganism counting and biovolume measurement, indicating that they are two different research topics.

1.3 Related Reviews

Due to the biovolume measurement is an essential topic in the research of microorganisms, plenty of literature reviews are published based on the abundant research, which are summed up as follows:

Bölter et al. [35] describes the research progress of microbial direct microorganism counting method, and discusses the technology and application of each direction from two aspects of microorganism counting and biovolume measurement. This review discusses data analysis and error propagation, which are widely neglected in the quantitative study of microbial ecology, and compares different microbial staining techniques and their applications. This review discusses the common staining methods and compares the advantages of each method. In this review, there are 3 papers are about calculating the error propagation and more than 23 papers are about biovolume measurement.

Qiu et al. [31] reviews the application of both size measurement and counting for bacteria. The automatic flow analysis technology and classical counting methods are introduced. At first, the plate counting method is the earliest developed method, then the immunofluorescence microscopic method and most probable number (MPN) are wildly used. With the development of computer technologies, DIP has shown the extremely convenience for microbial counting analysis. In the field of cell measurement, the different microorganisms can be detected and classified by using the water flow image method. However, the microorganisms with small size are difficult to be detected. The application of resistance change method can precisely measure the number and size of the individual cell, but the classification is difficult. Another measurement method with fast speed and high accuracy is flow cytometry. However, the concentrations of samples are limited to be high. There are more than 25 papers are summarized to illustrate the application of the size measurement of cell.

Gracias et al. [32] summarized the application of chromogenic and impedance method for microorganism classification and counting. The classical microbial measurement methods for food safety testing are illustrated. There are more than 28 papers are about microorganism measurement methods.

Daims et al. [33] describes the microbial quantification methods based on DIP. The material difference of microbial counting and microbial biovolume measurement is the identification of a single cell. Thresholding and edge detection are most widely applied methods by using DIP. And the development of local thresholding can focus on the region of interest and obtain the better segmentation result comparing with global thresholding. There are 6 papers are about automatic cell counting, 14 papers are about quantification of cell size and 11 papers are about biomass quantification.

Dazzo et al. [36] describes the application of CMEIAS (Center for Microbial Ecology Image Analysis System) computer-assisted microscopy for data extraction from images after accurately segmented, that can provide 63 different insights into the ecophysiology of microbial populations and communities within biofilms and other habitats. There are eight quantitative assessments topics are proposed, that are morphological diversity as an indicator of impacts that substratum physicochemistries have on biofilm community structure and dominance-rarity relationships among populations, morphotype specific distributions of biovolume body size that relate microbial allometric scaling, metabolic activity and growth physiology, fractal geometry of optimal cellular positioning for efficient utilization of allocated nutrient resources, morphotype-specific stress responses to starvation, environmental disturbance and bacteriovory predation,

patterns of spatial distribution indicating positive and negative cell-cell interactions affecting their colonization behaviour, and significant improvements to increase the accuracy of color-discriminated ecophysiology. More than 50 papers are used to describe quantification of biofilms.

Costa et al. [37] describes the development of biological wastewater treatment (WWT) using image analysis. This review introduces the fields of application of image analysis based WWT, such as aerobic wastewater treatment biological processes, calculation of sludge settling ability, measurement of sludge contents, detection of toxic compounds, biomass physiology analysis, full-scale WWT plants, aerobic granulation detection, quantification of the physical characteristics of the anaerobic granular sludge, analysis the behavior of anaerobic granules and biomass activity research. More than 110 papers are used to list the application of image analysis in WWT field but there is no definite description for microorganism counting or biovolume measurement, and there is no mention for technique methods.

Dazzo et al. [34] introduced the application of CMEIAS for microbial counting and biovolume measurement based on DIP. The shape-adaptable methods can be applied to measure the length and width of cell for the calculation of cell size. Then, a supervised tree is applied for individual cell classification. After that, a k-Nearest Neighbour (kNN) classifier is used to cluster the complex particles, such as spherical coccus and branched filament. Moreover, several parameters are calculated to location the spatial distribution of microorganisms in the biofilm. The extracted data can be analyzed by geospatial statistics, that is used to define the biogeography of microbial cells during the development of biofilm. And the colonization behavior models are generated by using the cell-to-cell interactions intensity. In the fourth part, the image segmentation algorithms are applied to show the color and spatial relationships of the foreground pixels. Finally, the applications of CMEIAS is summarized that contains the image analysis for morphological diversity, filamentous microbial morphotypes, ecophysiological attributes linked to accurate measures of biovolume body mass, spatial pattern analysis and its relationship to microbial biofilm ecology and color segmentation tool for cell-cell communication. More than 35 papers are about measurement of biovolume.

Li et al. [38] introduces the development of microbial analysis based on DIP and amounts of methods used for microorganism classification are summarized. In this survey, the microorganisms are grouped based on their application domains, including Agricultural Microorganisms (AMs), Food Microorganisms (FMs), Environmental Microorganisms (EMs), Industrial Microorganisms (IMs), Medical Microorganisms (MMs), Water-borne Microorganisms (WMs) and Scientific Microorganisms (SMs). They analyse the properties of the methods below and the practical conditions of the microorganism classification tasks jointly, the methods include image preprocessing methods such as image segmentation, feature extraction methods, post-processing methods, feature fusion methods and classification methods. More than 60 related papers are summarized to illustrate different microbial classification methods. This review is a comprehensive microorganism classification paper and uses plenty of literatures for quoting, but there is no significant description for microorganism counting or biovolume measurement.

The comparation of several related works and their contribution to biovolume measurement are shown in Fig. 5. It is observed from the previous studies that the explanations about the current technologies of microorganism research are objective and detailed. However, the targeted research about biovolume measurement is limited. Therefore, additional research on this aspect needs to be completed. Since microorganism quantification plays a vital role in microbial

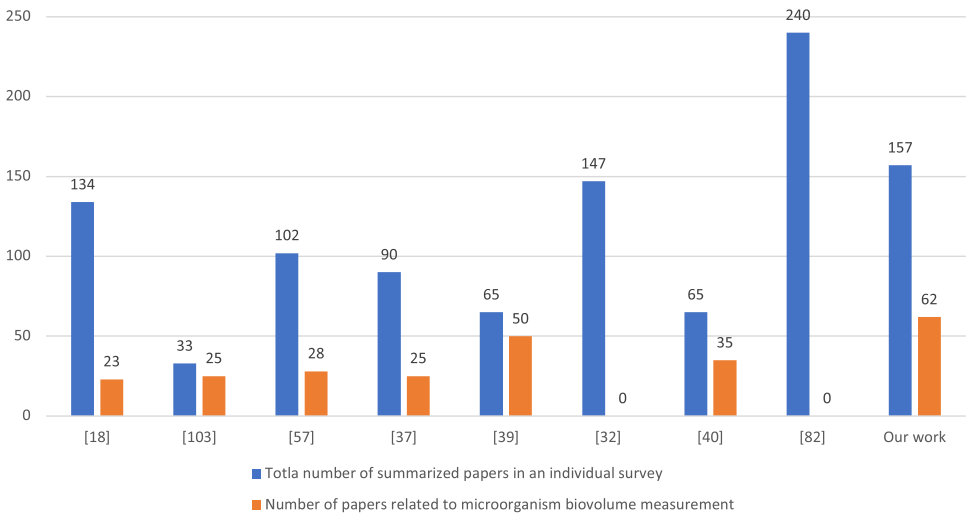

Fig. 5 The comparation of related survey papers. The related works are list with their contribution to image analysis based microorganism biovolume measurement

research, this review focuses on applying microorganism biovolume measurement, and the prospects of the methods. This review has high research significance and application value for microbiological researchers and computer vision researchers. There are more than 62 papers are summarized in this survey about biovolume measurement.

1.4 Microorganism Biovolume Measurement Methods

The flow chart of microbial biovolume measurement is shown in Fig. 6 to elaborate on the methods. The approach contains five steps: microbiological data acquisition, microscopic image, image preprocessing, microorganism biovolume measurement methods, and evaluation methods.

The microorganisms are composed of the following seven types according to the different application domains, including agricultural microorganisms, environmental microorganisms, food microorganisms, industrial microorganisms, medical microorganisms, water-borne microorganisms and other microorganisms. Then, the digital images are obtained after staining and slicing by using professional equipment [39]. The following part is pre-processing, including image denoising and contrast enhancement, which is helpful for image segmentation. The next step is biovolume measurement methods [40]. Biovolume measurement aims to measure the morphological parameters and calculate the biovolume. The most significant part of microorganism biovolume measurement is image segmentation. Finally, the evaluation methods are proposed. However, the results obtained in these studies are area and volume, that are difficult to be compared with the results obtained by manual methods. So the proper evaluation methods can help to analyze the performance of the image analysis methods [41].

1.5 Structure of This Review

This study proposes a comprehensive review of microorganism biovolume measurement using image analysis. The research of microbial application was first developed in 1980, and the articles, including research articles and review articles, are summarized. Moreover, the application of microorganism biovolume measurement in various circumstances are discussed. More than 62 papers are selected from the initial paper dataset, and the structure of the systematic review is shown in Fig. 7.

The review is organized as follows: In Sec. 2, the DIP and evaluation approaches, which are widely applied for microorganism biovolume measurement, are summarized. In Sec. 3, the relevant research on DIP-based microorganism measurement are grouped and summarized. In Sec. 4, the quantitative analysis of different DIP approaches for microorganism

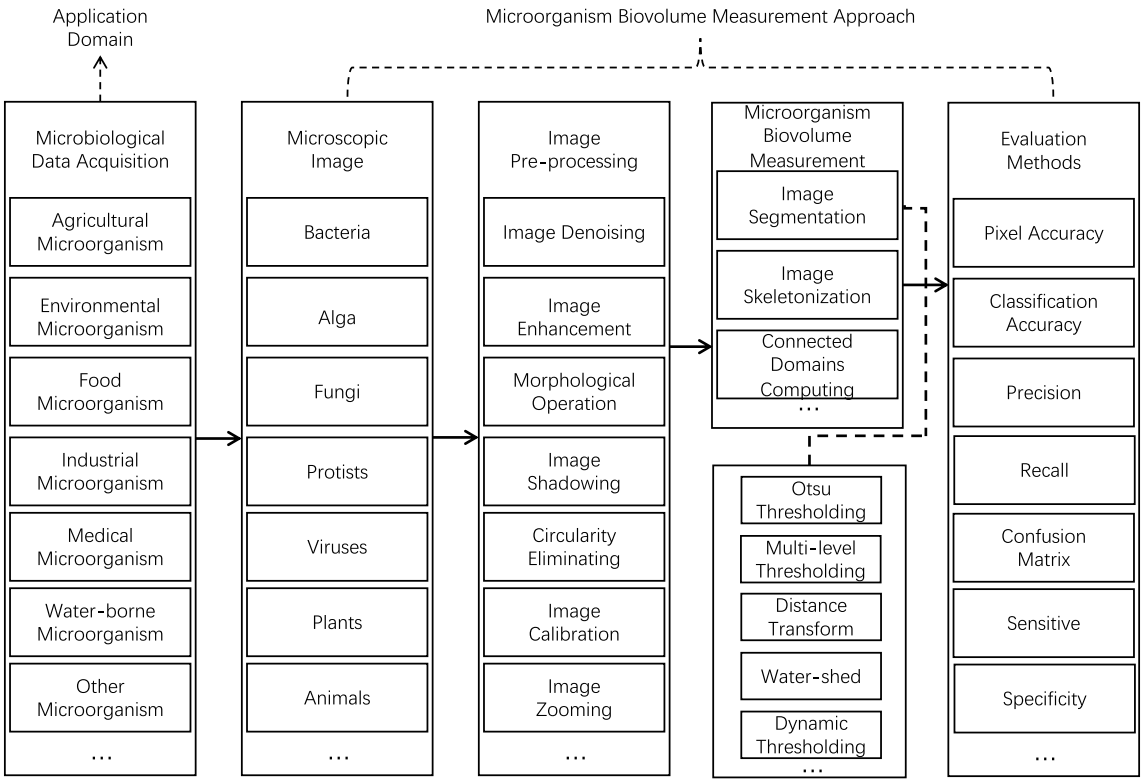

Fig. 6 The organisation chart of microorganism biovolume measurement approaches in this paper

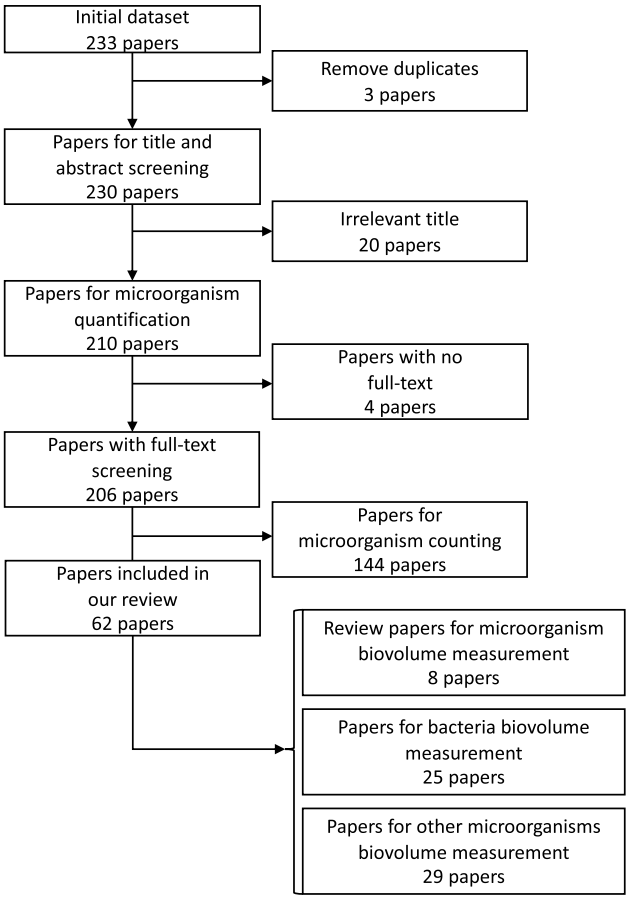

Fig. 7 The systematic flow chart of paper selection for our work

biovolume measurement is summarized. Then in Sec. 5, the commonly used approaches are summarized. Finally, in Sec. 6, this review is concluded by summarizing the whole paper. This review structure is clear enough to help researchers comprehend the DIP-based microorganism biovolume measurement's current situation.

2 Image Analysis Based Microorganism Quantification Methods

The application of DIP technology to microbial biovolume measurement can promote stability and higher accuracy by comparing it with traditional measurement. This chapter introduces the commonly used DIP technologies applied in microorganism biovolume measurement.

2.1 Image Analysis Technology

2.1.1 Image Pre-Processing

In the process of image generation and transmission, the image quality is often degraded due to the interference and influence of various noises, which will have a negative impact on the subsequent image processing and image visual effect. Therefore, in order to suppress noise and improve image quality, denoising methods need to be applied. The main methods to remove noise are spatial filter, transform-domain filter and so on. Spatial filtering directly performs data operation on the original image and processes the grey value of the pixel, such as the Median filter and low-pass filter [40]. The transform-domain filter contains Fourier transform and wavelet transform [42].

2.1.2 Image Segmentation

Image segmentation is an important method in digital image processing and computer vision, which contains threshold segmentation, edge detection and region extraction.

Threshold segmentation Thresholding is one of the classical methods for image segmentation, which has the advantages of simple calculation, high efficiency and fast speed [43]. The selection of the threshold is the core algorithm of threshold segmentation [44]. There are two main methods, the first one is iterative thresholding method, which can obtain the good results for the images with high global contrast [45]. Another one is the maximum inter class variance based on Otsu method, which can obtain the satisfactory result for most images [46]. This method is considered to be the best method for automatic threshold selection because it is easy to calculate and is not affected by the change of image contrast and brightness [47].

Edge detection based segmentation In the DIP, edge detection can reduce the amount of data and maintain the essential architecture of the image [48]. Edge detection includes gradient operator based method, second-order differential operator based method, LOG edge detection method and Canny edge detection method. The gradient operator based methods contain Roberts operator, Sobel operator, Prewitt operator, Kirsch operator and Robinson operator, which are the most widely applied for edge detection [49]. Sobel operator detection method has a good performance when image have a wide variety of noise, but the edge location is not accurate and the edge of the image is more than one pixel.

Region Based Segmentation Among the region extraction methods, watershed segmentation provides excellent results and widely used for segmentation. It belongs to a segmentation method based on region growth. The calculation process of the watershed is an iterative labeling operation, which is sensitive to feeble contours [50].

2.1.3 Morphological Operation

The commonly used morphological operations include dilation, erosion, close operation, open operation and so

on, which are usually applied in pre- and post-processing in DIP [51]. The satisfactory results can be obtained after morphological operations.

2.1.4 Morphological Features

The commonly used features in biovolume measurement consist area, perimeter, length and width. The area can be obtained by calculating the inner pixels, the perimeter can be calculated by counting the contour pixels. The length and width can be obtained from the features of the central axis [52].

2.2 Evaluation

Evaluation is an essential part of DIP, which can help researchers find the reasons that affect the result. True positive (TP), false negative (FN), false positive (FP) and true negative (TN) are four basic metrics in image classification. Commonly used evaluation metrics are shown in Table 1.

2.2.1 Classification Accuracy

Accuracy is the proportion of correctly classified samples from all samples [53]. TP, FN, FP and TN can be composed as confusion matrix [54]. The columns of confusion matrix are predicted results and rows are real classification. Precision is the probability of samples which are correct predicted from the predicted positive samples. Recall is the proportion of positive prediction from all positive samples [55]. F1-score is the weighted harmonic average of precision and recall [56].

2.2.2 Segmentation Accuracy

Pixel accuracy (PA) is a basic evaluation method in image segmentation, that is the proportion of pixels that are classified correctly. The mean pixel accuracy (MPA) is the improved methods of PA, which performs more objective [57]. Dice is applied to measure the inner similarity between segmented image and GT [58]. Intersection over union (IoU), also named Jaccard, is the proportion of intersection and union of the prediction and ground truth [59].

Evaluation is one of the most essential parts of DIP, which is the performance measurement of the model. The results of evaluation can affect the performance of microorganism biovolume measurement directly.

3 Microorganism Biovolume Measurement Methods

Microorganisms come in various types, and different microorganism biovolume measurement methods show different performances. The microorganism biovolume measurement methods are suitable when colonies are adherent. In this chapter, the current applications are summarized and structured as follows: firstly, the semi-automatic methods, gray level histogram methods, thresholding methods, morphological methods, edge detection methods, and third-party tools for bacteria biovolume measurement are summarized. After that, the image enhancement-based methods, thresholding methods, machine learning-based methods, edge detection-based methods, region connection-based methods, morphological methods, and third-party tools methods of other microorganisms measurement methods are summarized, including animal, alga, plant, fungi, spore, virus, and protozoa.

3.1 Bacteria Measurement Methods

Bacteria is one of the essential parts of microorganisms, and the datasets of bacteria are relatively abundant, which are usually used in microbial research.

3.1.1 Bacteria Measurement Methods Based on Semi-Automatic Operation

In [60], an scanning electron micrograph based dialogue program is developed. The system needs users to mark the width and length of all bacteria and then calculates the

Table 1 The definitions of evaluation metrics for image classification and image segmentation

Metric	Definition	Metric	Definition
Accuracy	$\text{Accuracy} = \frac{TP+TN}{TP+TN+FP+FN}$	Precision	$\text{Precision} = \frac{TP}{TP+FP}$
Recall	$\text{Recall} = \frac{TP}{TP+FN}$	F1-score	$\text{F1-score} = \frac{1}{\frac{1}{\text{Precision}} + \frac{1}{\text{Recall}}}$
PA	$\text{PA} = \frac{\sum_{i=0}^{k} P_{ii}}{\sum_{i=0}^{k} \sum_{j=0}^{k} P_{ij}}$	MPA	$\text{MPA} = \frac{1}{K+1} \sum_{i=0}^{k} \frac{P_{ii}}{\sum_{j=0}^{k} P_{ij}}$
IoU	$\text{IoU} = \frac{TP}{FN+TP+FP}$	DIce	$\text{DIce} = \frac{2TP}{FN+2TP+FP}$

biovolume increment of bacteria. The total time required could be reduced from 1 day to 2.5 h by using a M6520 microcomputer program.

3.1.2 Bacteria Measurement Methods Based on Gray Level Histogram

In [61], the mean value of the RGB histogram and the ratio of red to blue intensity components are used to determine the concentration of bacteria biomass. The sum of the mean values of the RGB distributions are linearly related to the total biomass protein concentration.

In [62, 63], biofilm is applied for reconstruction and quantification of bacteria biovolume. First, a median filter [62] and contrast stretching [63] are applied for noise reduction, and then the image contrast is enhanced by using histogram stretching. After that, the method of histogram equalization and a high pass filter [63] is applied to enhance images. In [62], the dead biofilm patches are eliminated by comparing the patch morphology with substrate morphology, and three metrics are then computed for the individual biofilm patches: patch area, patch perimeter, and circularity, which can be applied for bacteria colony biovolume measurement. The result shows that the patch morphology is useful for investigating the relationships between surface morphology with biofilm growth and determining the surface morphology and biofilm shape. In [63], the geographical information systems (GIS) are used to reconstruct the biofilm images and measure the biovolume of bacteria. The 3-D reconstruction of the bacteria volume is shown in Fig. 8.

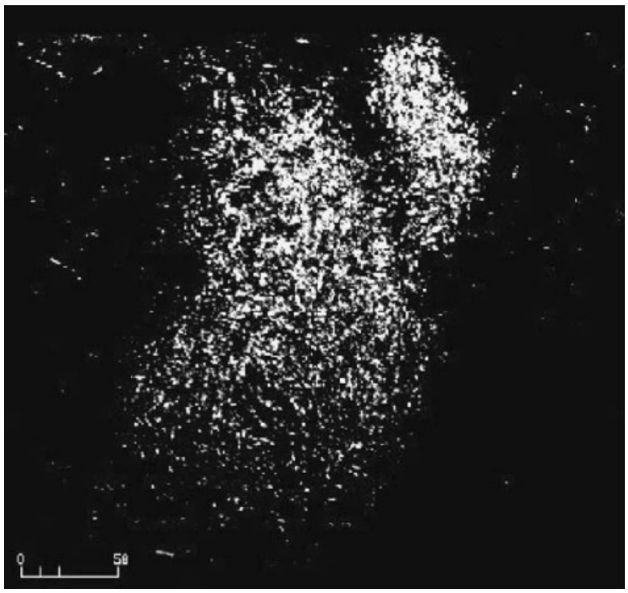

Fig. 8 The 3-D reconstruction image of the biovolume, which is obtained based on the five biofilm sections (In [63] Fig. 6)

3.1.3 Bacteria Measurement Methods Based on Thresholding

In [64–66], thresholding is applied for bacteria biovolume measurement. First, contour enhancement [64] is applied for pre-processing. Then the thresholding methods with fixed value are applied for determination of bacteria biomass. The system can detect and measure the objects after segmentation and erosion operation, which provides estimates of cell number, mean volume and biovolume with standard errors of about 5%. In [65], the connected-volume filtration can erase debris outside the region of interest after thresholding. Finally, the quantity of elements can be measured. In [66], the useless particles are removed after thresholding segmentation. Then the wavelet transformation and densitometric techniques are applied to quantitatively estimate the growth of cells. The measurements of densitometric techniques are based on the measurements of the area occupied by the cells, the maximum and average cell grey-scale tones. It shows the predominance of larger wavelet coefficients for the images with a higher biomass content or number of cells. The processed images are shown in Fig. 9.

In [67, 68], Otsu Thresholding is applied for bacteria biovolume measurement. Both methods use confocal laser scanning microscopy (CLSM) images of bacteria for quantification. First, Otsu Thresholding is applied for CLSM images segmentation. Then in [67], the parameters of biofilm are obtained by calculating the binary image stacks with connected volume filtration (CVF). The number of fore-ground pixels are multiplied by the volume of voxel in a stack, that represents the biovolume. The volume of voxel is the square of the pixel size multiplied by the scanned step size. In [68], the color channels are connected with the connected volume filtration matrix (1 = connected-biofilm bacteria and 0 = either unconnected bacteria or background noise) after Otsu Thresholding. The same pixel location of dead and live bacteria is compared. If both live and dead channels are 1, the dead channel remains 1 and the live channel converts to 0. Moreover, if the CVF matrix has the same value as the color channel, this pixel is labeled as connected bacteria. On the contrary, if the value of color channel is one, but the CVF matrix has a value of 0, the particular pixel is labeled as unconnected bacteria. Furthermore, if the CVF matrix has the same value of 0 as the color channel, this pixel is labeled as noise. Finally, the green and red channel points are summed up to calculate the percentage of dead and live bacteria populations. The result is shown in Fig. 10.

In [69], the adaptive thresholding is used to determine the structure of bacterial biofilm. The images of bacteria

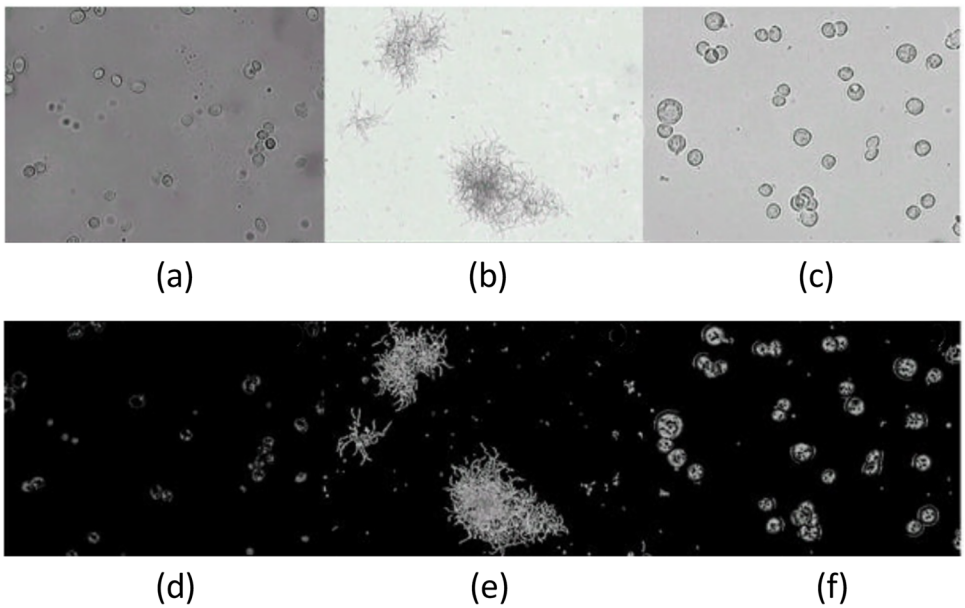

Fig. 9 The original and processed images. **a** Yeast; **b** bacteria; **c** insect cell; **d** processed image of yeast; **e** processed image of bacteria; **f** processed image of insect cell (In [66] Fig. 5)

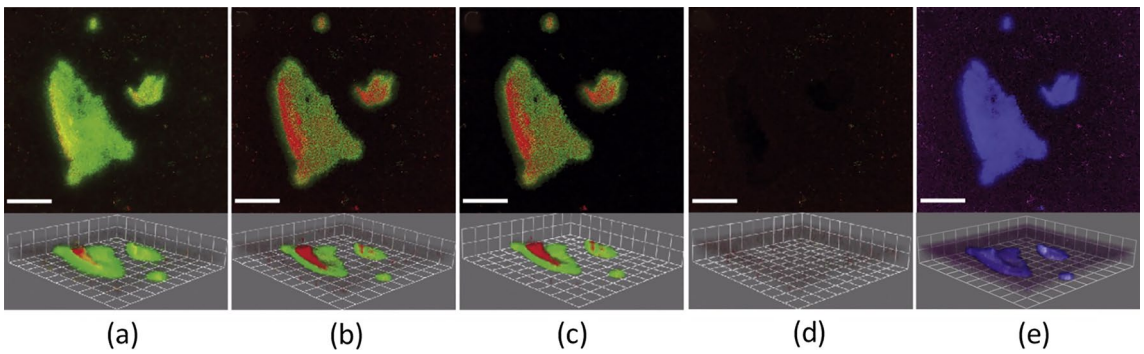

Fig. 10 The result images after processing (In [68] Fig. 4)

biofilm are obtained using CLSM, then an adaptive thresholding is used for image segmentation. Finally, the image structure analyzer is used to extract the features of biofilm and the thickness of biofilm is calculated for biovolume quantification.

3.1.4 Bacteria Measurement Methods Based on Morphological Operation

In [70], an image analysis system is used to determine the biovolume of filamentous bacteria. The image processing program consists of three stages: image pretreatment, segmentation and debris elimination. Finally, the morphological parameters are measured to calculate the total recognized aggregates area per volume, the number of recognized aggregates per image, percentage number of recognized aggregates and recognized aggregates area percentage.

In [71], the images are separated into three types that contains cocci, rods and others, then different formulas are used to calculate the biovolume of each type. The integration of volume performs better than simple addition.

In [72], more than 30 biofilm samples are captured for measurements of several parameters, such as the area of biosurface, biovolume, and biothickness. After that, the biofilm area on each slice is obtained for measurement of biovolume. The stack of 39 biofilm images in a 15-μm biofilm is shown in Fig. 11. Finally, the measurement of the area can be obtained by calculating the heterogeneous growth.

3.1.5 Bacteria Measurement Methods Based on Edge Detection

In [73], the contrast of images are enhanced and the channel is separated into blue and green. Then, the Marr-Hildreth filter is used for the detection of objects in green channel. After that, the useless debris are removed. Finally, the area and fiber length of fungi and bacteria in the gut of earthworm are measured.

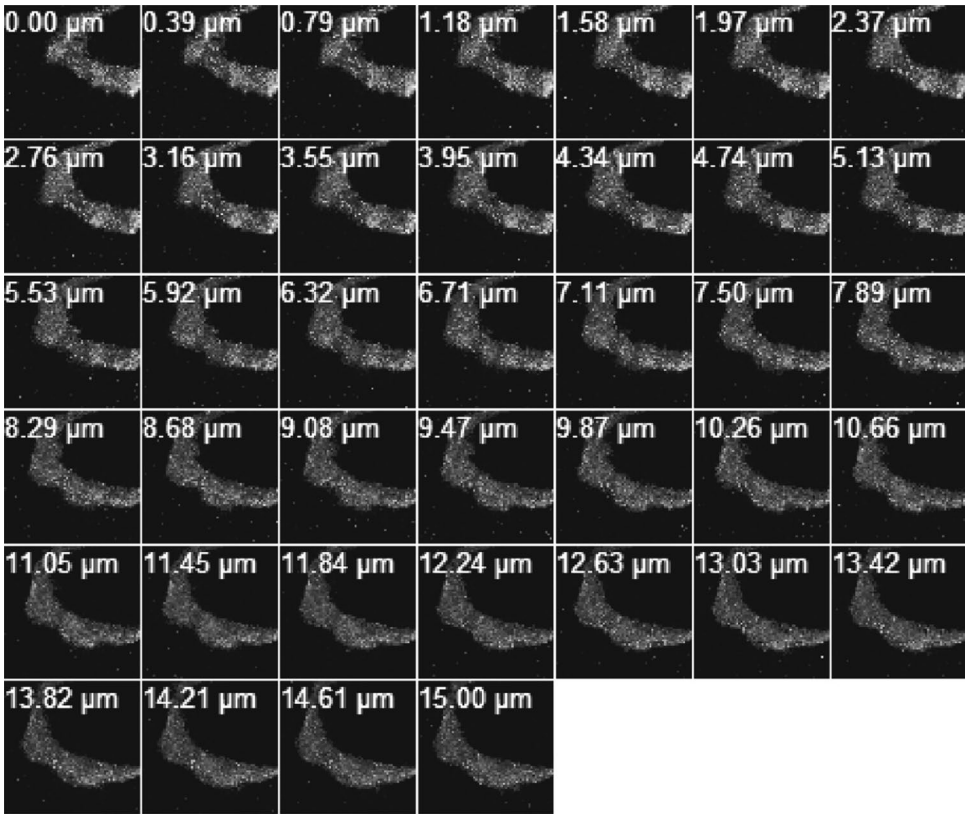

Fig. 11 The biofilm images captured by CLSM (In [72] Fig. 3)

3.1.6 Third-Party Tools

In [74], the marine microorganisms are measured by using the 'Artek 810' image analyzer (Artek Systems Corp.,Farmingdale,N.Y.), and a variable gray-level is set to obtain the binary images. The area and perimeter are measured to estimate the abundance of marine organisms.

In [75–78], the 'IBAS' (Kontron Inc., Eching, West Germany) series image processors are applied for biovolume measurement of bacteria. In [75, 76], 'IBAS 2000' image processor is applied to measure the area of darkfield bacteria images [75],microcolony count, area and size distribution [76] by enhancing the cell contrast. The moving objects can be highlighted using the motility of bacteria difference images of exercised images with initial images. The result shows that computer enhanced microscopy (CEM) is better than direct microbial observation in terms of speed, precision, and quantitative data collection. In [77], the intensity changing is corrected by using a low-pass filter. Then, 'IBAS 2000' is used to count the *Staphylococci* and calculate the surface area. In [78], discriminate the area using different threshold after contrast and contour enhancement, and then the 'IBAS II' is applied to calculate the total particulate matter area of copepods.

In [79], the morphological processor is used to enhance the bacteria image and the 'Quanitmet 570' computer system (Leica, Cambridge, United Kingdom) is used for image processing. Then images are binarized using threshold and the calculation of biovolumes is guided by a numerical integration method by following the trapezoidal rule.

In [80], 'Image Pro Plus version 4.5' is used for quantification of bacteria. The cluster of bright pixels can be recognized as cells, whose area can be measured automatically by using 'Image Pro Plus'. The data is stored as normalized accumulated distribution of cell. Finally the cumulative cell distribution is measured.

In [81], 'bioImage_L' is used to determine the baseline physiology of dental plaque grown in a mini-flow cell system. First, the CTC (red) and Syto24 (green) are used to stain the biofilm image. Then, a Gaussian low-pass filter and Otsu Thresholding are applied for image segmentation. After that, the green channel and red channel are reconstructed in three dimensions that is shown in Fig. 12. Finally, the biovolume of dental plaque is measured and the results on the viability of dental plaque bacteria indicates that the biovolume of the subpopulation of microbes with undamaged cell membranes accounts for 96% $\pm$ 2% of the total biofilm biovolume.

In [82], 'ImageJ' v1.41 (US National Institutes of Health) is used to determine the total biomass and the individual biomass. The calculation of total biomass is the sum of all living cells biovolume, and the individual biomass is the biovolume of single cell. Once the CLSM images are obtained, the ImageJ v1.41 software is applied for green and

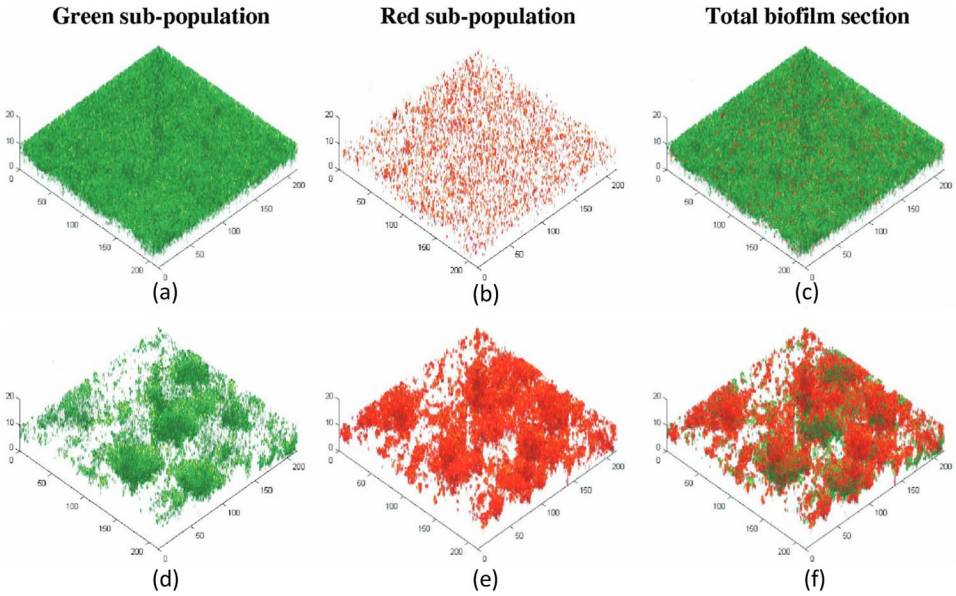

Fig. 12 Reconstructions of dental plaque biofilms, image (**a**) to (**c**) are cultivated on a polystyrene surface, and image; **d** to **f** are cultivated on a saliva surface (In [81] Fig. 2)

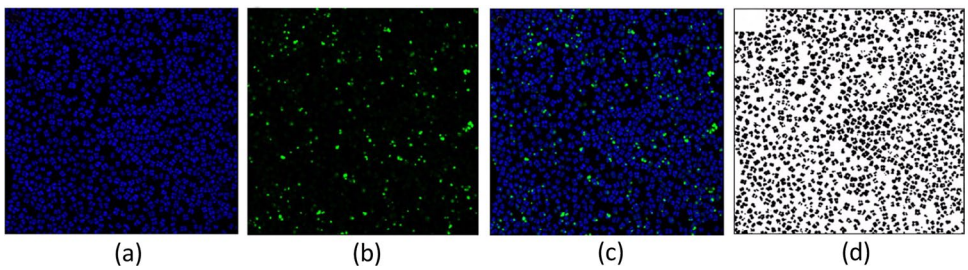

Fig. 13 The process of image analysis for CLSM images (In [82] Fig. 1)

blue pixel enumeration of each image. Then the images are transformed to binary images using an automatic threshold. The final fluorescence image of blue channel is determined by subtracting the green channel from initial image, on the contrast, the fluorescence image of green channel is determined by subtracting the blue channel from the initial image. Then the image is smoothed by median filtering. The ratio of the blue or green threshold voxels to the total threshold voxels can represent the ratio of live and dead cells. Finally, the biovolume of bacteria is measured and multiplied by a conversion factor to convert it to biomass. The process of image analysis is shown in Fig. 13.

In [83], the 'ImageJ' and 'CellC' are applied for bacteria counting in ballast water. The size and shape of individual cells or the intensity of fluorescently labelled microorganisms are measured with quantum dots or fluorochromes. The user can adjust the parameters of the modules in software to adapt various experimental environments, then the measurement results can be obtained from hundreds of images.

In [84], the CMEIAS, which is proposed in [85], is used for biovolume measurement. The shape and morphological features are extracted by using CMEIAS to calculate cellular biovolume. The accuracy and error rates are calculated, which contains seventeen distinct methods for calculation biovolume by comparing with the ground truth using DIP. It is proved that this improved technology of biovolume measurement has high accuracy in the determination of the selection of algorithm, which is applied for biovolume computation of morphologically diverse communities captured by classical microscope at single cell resolution.

3.1.7 Summary of Image Analysis Based Biovolume Measurement for Bacteria

By reviewing the works of image analysis based on bacteria biovolume measurement and referring to Table 2, we find that:

– Development trend: The development of image analysis methods based on bacteria biovolume measurement started in the 1980s and developed rapidly in the 2010s, showing the increasing importance of bacteria research in human society. With the continuous improvement of DIP and pattern recognition, the bacteria biovolume

Table 2 Summary of image analysis based biovolume measurement for bacteria

Related work	Microorganism	Pre-processing methods	Segmentation methods
[60]	Bacteria		Width and length marking
[64]	Bacteria	Contour enhancement	Thresholding
[71]	Bacteria		Thresholding
[65]	Bacteria	Connected-volume filtration	Thresholding
[62]	Bacteria	Median filter and histogram stretching	Thresholding
[70]	Bacteria	Morphological parameters measurement	Thresholding
[61]	Bacteria		RGB histogram segmentation
[73]	Bacteria	Contrast enhancement, morphological operations and thresholding	Marr-Hildreth filter
[63]	Bacteria	Contrast stretching, histogram equalization and high pass filter	Geographical information systems
[66]	Bacteria	Thresholding	Wavelet transform and densitometric techniques
[67]	Bacteria		Otsu Thresholding
[72]	Bacteria		Stack superficial area measurement
[69]	Bacteria		Adaptive thresholding
[68]	Bacteria	Connected volume filtration	Otsu Thresholding
[74]	Bacteria		Artek 810 image analyzer (Artek Systems Corp.,Farmingdale,N.Y.) and gray-level converting
[75]	Bacteria		IBAS 2000 (Kontron Inc., Eching, West Germany)
[76]	Bacteria	Contrast enhancement	IBAS 2000 (Kontron Inc., Eching, West Germany)
[77]	Bacteria	Low pass filter	IBAS 2000 (Kontron Inc., Eching, West Germany)
[78]	Bacteria	Contour enhancement	IBAS II
[79]	Bacteria	Morphological processor	Quanitmet 570 computer system (Leica, Cambridge, United Kingdom) and thresholding
[80]	Bacteria		Image Pro Plus version 4.5
[81]	Bacteria	Gaussian low-pass filter	BioImage_L and Otsu Thresholding
[82]	Bacteria	Median filter	ImageJ v1.41 (US National Institutes of Health)
[83]	Bacteria		ImageJ and CellC
[84]	Bacteria		CMEIAS

measurement approaches will have appreciable development in the future.
– Measurement techniques: The medial filter and contrast enhancement are the most frequently used pre-processing method. Image segmentation methods are thresholding and Otsu thresholding.

3.2 Other Microorganism Measurement Methods

3.2.1 Measurement Methods Based on Image Enhancement

In [86], the 'Equalize/Best fit' method is used to enhance the contrast of phytoplankton images for obtaining good detection of filaments. The measurement of biovolume is determined by the volume calculation of a cylinder, which contains measurement for trichome and section of trichome. The diameter represents the minimum diameter and the length represents the maximum diameter.

3.2.2 Measurement Methods Based on Thresholding

In [18, 87–91], thresholding approaches are applied for microorganism biovolume measurement. First, a median filter [89], contour enhancement and contrast enhancement [88] are applied for denoising and image enhancement. Then, the local adaptive background correction [89] is used for spatial threshold changing, which caused by the inhomogeneity of the illumination and fluorescence while imaging. After that, a high-pass filter 'Black tophat' [90] is used to extract black detail from a background with variable intensity. In [18], a threshold is used to remove the background and the lines of fungi images are enhanced, then thinning operation is used to keep the hyphae into one-pixel width and calculate the total length. The manual method and automated method have obtained very close results. In [87], a

threshold is used to convert grey images into binary images. The average particle thickness is used to convert the area (two-dimensional) into biovolume (three-dimensional). The resulting linear relationships are found to be significant in homogeneous samples like the spheres and diatoms. In [88], thresholding is used to separate the colony from the background and then the features are extracted. Then the area and biovolume of colony are calculated. The result shows that image processing method can be applied in interface cultivation to measure the growth conditions of colony. In [89], thresholding is used to quantify the plankton and improve the accuracy of measurement. The images are automatically segmented into filaments and background by binarization with a single intensity threshold. After that, the segmented images are thinned and the total filament length is measured. The result shows that the filamentous bacteria can be quantified automatically, that has high accuracy and robustness. In [90], a thresholding based method is used for automated measurement of filamentous cyanobacteria. The holes within the object are filled after thresholding. Finally, the parameters such as area and perimeter of all particles are measured, which are applied for the calculation of curve length and curve width. By comparing with the manual measurement procedure, the error of filament length calculations is less than 1%.

In [91], digital image processing is used for quantification of alga. First, the RGB images of alga are obtained form a CCD camera. The color in RGB channel of region of interest (ROI) are segmented and filtered by using two algorithms. The colored images are converted to gray-level images in first algorithm and the weights of RGB channels are obtained separately. Then the second algorithm is applied for color feature extraction. Finally, the densities of cell are calculated and the correlation coefficient between the method and manual measurement method is 0.997.

3.2.3 Measurement Methods Based on Machine Learning

In [92], an artificial neural network is applied for algal biovolume measurement. First, a neighborhood-averaging filtering method is used to remove the noises of algal images. The filtered light distribution image is converted to a contour image by grouping the original 8-bit gray scale into a desired value. Then, an artificial neural network model is used to relate the cell density in the photobioreactor with the digitized images. The present study shows that image analysis techniques can be used to measure light intensity in a photobioreactor, and then the cell concentration in a photobioreactor can be predicted with high accuracy by analyzing the image data using a neural network model.

In [93], SVM is used for plankton biovolume estimation. First, SVM is applied for plankton classification. Then, three methods are designed for biovolume measurement. In the first method, for the spherical shape particles, the projected area of each object is applied for biovolume calculation. In the second method, the measurement of biovolume is considered as the calculation of a evolution volume, which is designed manually, and then the width and length are measured for calculation. In the third method, the particles are classified based on shape features and DIP is applied for biovolume measurement. The accuracy of proposed method for plankton classification can be improved up to 86%.

In [94], an automatic cyanobacterial quantification system is developed using pattern recognition and machine learning. First, the initial images are denoised and the regions of interest are extracted, which have seven main steps. First, adaptive brightness and contrast adjustment are applied for exposure minimization. Then a Sobel based bidimensional convolution is used for contrast enhancement. After that, thresholding is applied to convert images to binary images for enhancement of connected elements in the image. Moreover, contours closing and holes filling are applied to extract explicit parts from all closed shapes. The noises and spurious objects are erased to reduce computational complexity, and the objects with low roundness value are eliminated based on roundness filter. Finally the extracted objects are thinned and pruned for debris elimination. After image processing, the filamentous objects in the image are processed as several points. And the crossing and interrupted filaments are recombined for accurate measurement. Afterwards, the parameters of filament are measured and 17 parameters are selected for machine learning based on a Random Forest. The proposed method is shown in Fig. 14.

3.2.4 Measurement Methods Based on Edge Detection

In [95], the higher order local autocorrelational masks are used to extract plankton with their contours. The canonical correlation analysis is used to determine the area of plankton after plankton classification. The result shows that this method can measure the size of all plankton in the image with not contour labelling.

3.2.5 Measurement Methods Based on Region Connection

In [96], image analysis is used to estimate the cell density and biomass concentration of fungi. First, the total difference between background and foreground are minimized to obtain the threshold, that allows satisfactory result while adjusting for variations in background intensity. After that, an octagonal filter is applied for region connection, which can help to remain the tiny objects after subsequent denoising operations. Then the height and width filter are applied to remove fungi clumps. Finally, the 50 measured values of mycelium width in the stochastic selected images are

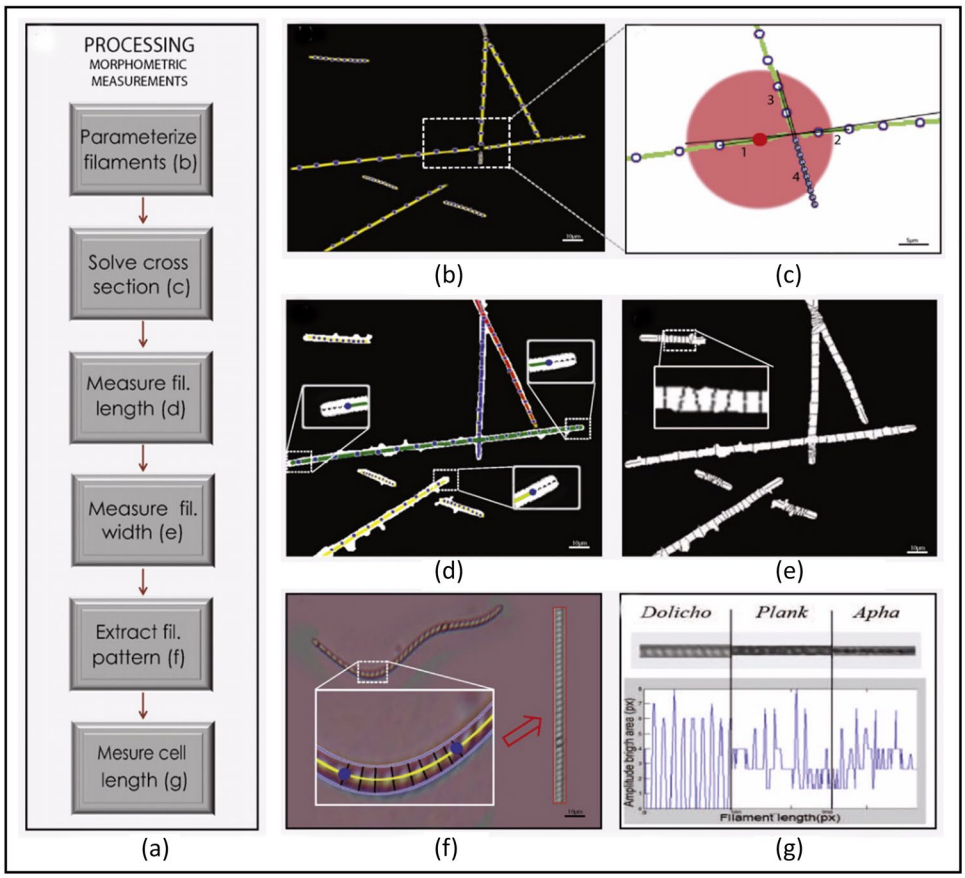

Fig. 14 Processing algorithm-morphometric measurements (In [94] Fig. 2)

averaged to estimate the cell diameter. The process of image analysis method is shown in Fig. 15.

3.2.6 Measurement Methods Based on Morphological Operation

In [97], DIP is used for determine the biovolume of cyanobacteria. The biovolume of aggregates is calculated by dividing the whole aggregate area with average area in the same image. As for curved and coiled filaments, the images are segmented to obtain the straight parts. Then the biovolume of images are calculated and added with other measurement results, that is used for determination of total biovolume of cyanobacteria.

In [98], quantitative image analysis is applied for quantification of microorganisms in waste water. Firstly, the binary images of the biomass of aggregate and the filamentous bacteria are obtained by using DIP, which contains image preprocessing, image segmentation and denoising. Then, the size of biomass of aggregate and filamentous bacteria are calculated by using this DIP system from the binary image obtained. The biomass of aggregate can be calculated by using the projected area, and the filamentous of biomass can be measured by using the total filament length.

3.2.7 Third-Party Methods

In [99], 'NIH-Image 1.62' (National Institute of Health, Bethesda, Md., USA) image analysis system is applied for biomass and biovolume determination of zooplankton. The major and minor axis of individual cell are measured and the corresponding volumes of the revolution ellipsoids are calculated. The proposed method can accurately estimate the biovolume and number of zooplankton based on DIP.

In [100], a digital image analysis software called 'Micro-Image 4.0' (Media Cybernetics for OLYMPUS) is used for fungi measurement. The median and high-pass Gauss filter are used to remove noises. Then the images are segmented in HSI channel and the projected areas are estimated. Moreover, the weighed mean value of segmented region to total area are calculated as the zone fraction. The result shows that the digital image analysis of *R. oligosporus* hyphae can obtain the fast and accurate segmentation results.

In [101], 'KS400 software' (Kontron Electronic GMB, Carl Zeiss MicroImaging, Inc., Thornwood, NY) is used to measure the biomass growth of fungi. A high pass filter is used to obtain the binary images, then the binary filters are used to obtain the features of images for biovolume measurement. In [102], 'KS400' is used for monitoring the biomass growth of fungi. First, the binary filters are applied to obtain

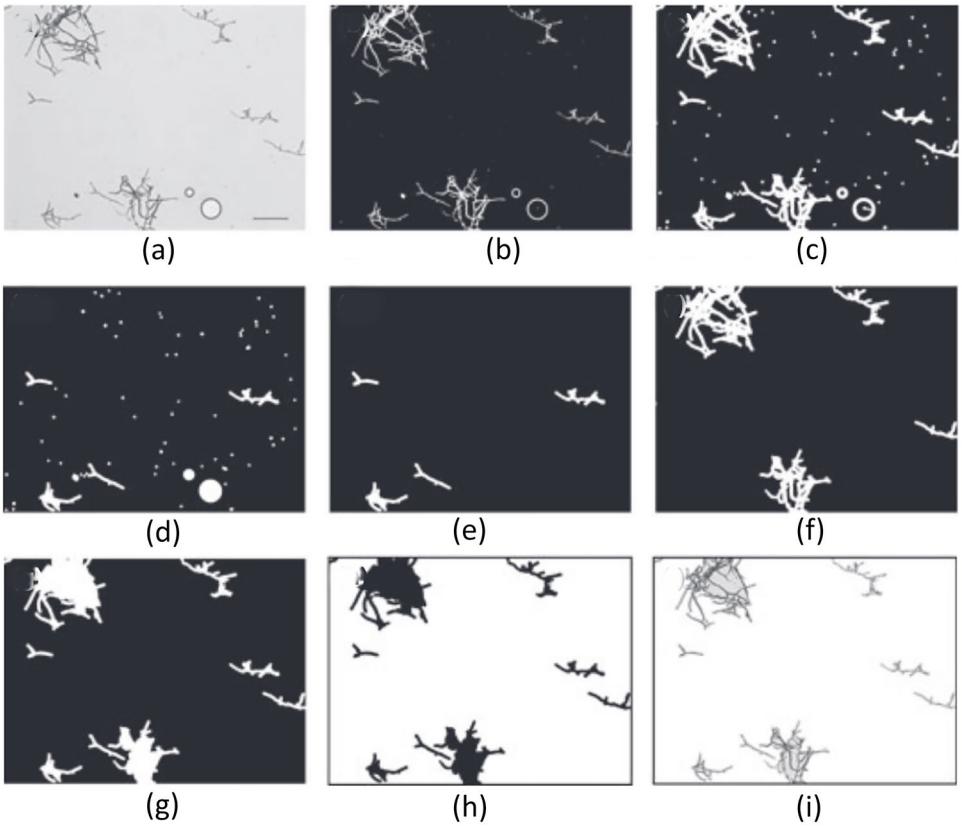

Fig. 15 The processing steps of image analysis system for area determination of fungi (In [96] Fig. 2)

morphological data. After that, a high-pass filter is applied to enhance the contrast of boundaries, and the images is binarized by using a fixed threshold. Finally, the debris are pruned and the biovolume are measured.

In [103], 'ImageJ' v1.33f (US National Institutes of Health) is used to determine the biomass of cyanobacteria based on image analysis. The threshold is calculated by 'ImageJ' that can separate the cyanobacteria clearly and then measure the biomass of cyanobacteria. It can be observed the significant differences between the manual measurement method and the proposed method ($p < 0.001$), with a 95% confidence interval (2.31, 4.14). The results show that the proposed method has higher accuracy when comparing with traditional manual method, particularly when the filamentous of samples have high density. In [104], 'ImageJ' is used for quantification of filamentous fungal. Firstly, the uneven illumination is adjusted by filtering. Then, the image is converted to a 2-dimentional signal and the high-pass filtering is applied to correct the background greyscale changes. After that, the gray-level threshold is calculated by 'ImageJ' and applied to obtain the binary image. Then the watershed algorithm is applied to separate the clustered objects and a single binary close operation is applied to erase any tiny crevices of images. Finally, the image is skeletonized and measured for determination of biovolume. In [105], 'ImageJ' 1.37v is applied to determine the biomass of cyanobacteria. First, a total of 4103 confocal images corresponding to 156 stacks were obtained. Then the threshold is used to transform to binary images and the ratio of the biovolume of object to sediment are calculated. To determine the individual biomass, a type of cyanobacteria in the stack is eliminated separately. Finally, each stack of biomass is measured.

In [106], the image analysis software 'LUCIA G/F' (Laboratory Imaging) is used for the measurement of the size and morphological features of microorganisms. There are two channels are used to correct possible pixel shift that caused by different excitation wavelengths. The first one is designed to detect DAPI stained particles by using UV-excitation, and another one is designed to detect hybrid bacteria by using blue excitation. Then, the 'AND' operation is applied for combination of binary images obtained by two channels. After that, a 'Mexican Hat' type edge detection filter is applied and the morphological operations like 'opening' and 'eroding' are applied to decrease the size of particles of processed image. Finally, the morphological parameters are measured for determination of biovolume.

In [107], 'Scion Image' 4.0.2 is used for quantification of alga. Thresholding is used to obtain binary image. After that, the area that covered by algae is dividing by the area of total image, which is calculated to represent the percentage area of alga. The number of zero pixels can be counted to quantify the area of the specific color channel in the binary image. Finally, the total number of chlorophyll is compared with the obtained result to verify the accuracy of this system.

In [108], 'ZooScan Integrated System' is used for quantification of zooplankton and the regression between image parameters with biovolume is obtained. The segmented image obtained by 'ZooScan' system is used for measurement of 46 different parameters including size, shape, gray level and the fractal dimension. The area is calculated with the size of the projection on a horizontal plane while the volume is calculated by assuming the shape of zooplankton is spheroid.

In [109], AutoCAD is applied to create the digital models of phytoplankton, then the parameters including volume and mass of object can be measured. Firstly, the cross-sectional outline of the phytoplankton images is detected. Then, the outline is revolved around the central axis to create the diatom disc. After that, holes are removed from the disc to meet the real distribution of areolae. Finally, other structural components of the phytoplankton are added. The creating process of 3D-model is shown in Fig. 16. Moreover, nine representative 3D-models are created in different size. To measure the biovolume of the phytoplankton, the proposed models are fit with a regression model to get the mathematical parameters of biovolume measurement.

In [110], Opera Phenix software is applied for imaging and measuring the biovolume of phytoplankton. After data acquiring, the images are processed in two methods. First, a 3D projection is rendered from the discrete confocal images, and the software can measure the biovolume of detected region of cells. Second, a 2D projection can be converted from the confocal images, which has the same view of a light microscope. Finally, the biovolume of phytoplankton can be measured.

In [111], Blender 2.79 is applied to create the 3-D model of algae and measure the biovolume. After modelling, a software tool, NeuroMorph, is applied to measure the area of the surface by calculating all area of each quadrangulated polygon of the mesh. Finally, the biovolume can be calculated.

In [112], Minitab version 16 (Minitab Inc., USA) is applied to determine the biovolume of *Mycoplasma fermentans*. First, a median filter is used for noise removing in each slice of images. Then, the filtered images are segmented based on thresholding to separate the microcolonies and realize the visualisations of 3D iso-surface. After that, Amira, version 5.4 software (Visualisation Sciences Group, USA), is applied to measure the biovolume of attached biofilm cells. Finally, MATLAB (Version R2013b, The MathWorks Inc., USA) is applied to measure the holes between cells. The measurement of channel diameter sizes is shown in Fig. 17.

In [113], the biovolume estimation of cyanobacterial colonies by using NeuroMorf software is compared with the other two methods. The first method is the traditional microorganism counting determined by experts. The second one is based on morphological approach, measuring the sphere packing, cell size and cell distance. Then, an approach based on regression is applied to calculate the relationship between cell number and the result of biovolume measurement. The ration between the measured biovolume using estimating and 3D modelling can be applied as the bias of estimation. Finally, ordinary least square analysis is applied to study the relationship between the colony volumes and overall cell biovolume in the colonies.

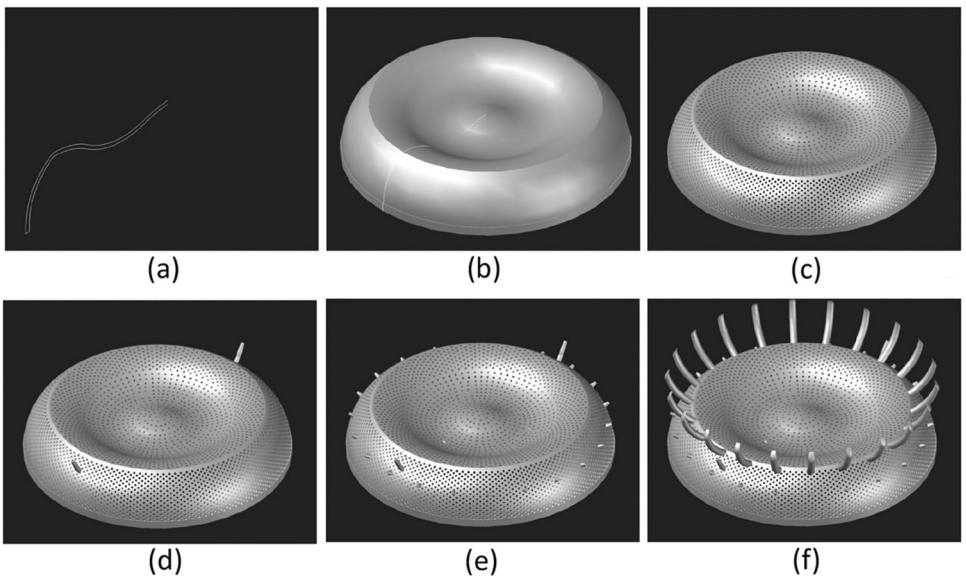

Fig. 16 The creating process of 3D-model for phytoplankton biovolume measurement (In [109] Fig. 2)

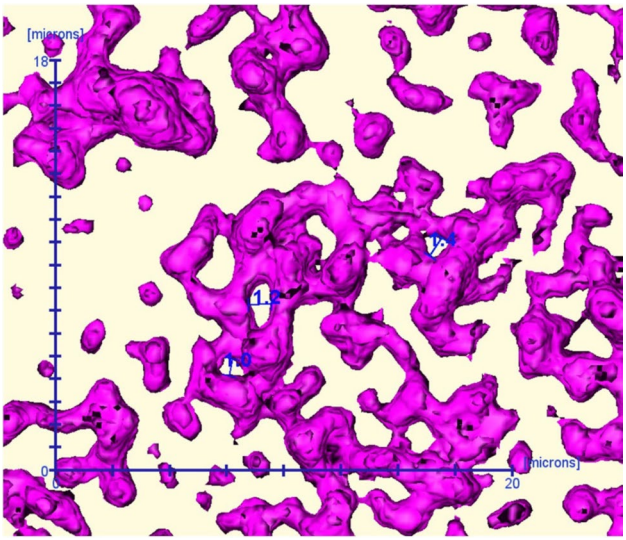

Fig. 17 The result of determining channel diameter sizes (In [112] Fig. 5)

3.2.8 Summary of Image Analysis Based Other Microorganisms Measurement

By summarizing the relevant research on DIP based on other microorganism's biovolume measurements and referring to Table 3, it can be seen that:

- Development trend: The DIP-based measurement for other microorganisms methods began in the 1980s and developed in the 2000s. It can be seen that the researches on other microorganism biovolume measurement have a similar development trend to related research on bacteria. However, bacteria research is relatively abundant and comprehensive, which may be caused by the limited dataset of other microorganisms such as fungi, alga, and viruses. On the other hand, compared with the hyphae of alga, bacteria have a relatively simple structure, which makes it challenging to segment completely.
- Measurement techniques: The most frequently used pre-processing method are the medial filter and contrast enhancement. Image segmentation methods are thresholding and Otsu Thresholding.

4 Quantitative Analysis of Microorganism Biovolume Measurement Methods with a Benchmark Dataset

In order to compare the performance of the DIP approaches mentioned above for microorganism biovolume measurement, a benchmark database is applied for the experiment of quantitative analysis. There are few open-source databases of the microorganism with adherent mycelia [114]. Therefore, we downloaded and adjusted the yeast database proposed in [115] to meet the requirements of biovolume measurement. An image with and without a mask and an adjusted mask of the yeast database is shown in Fig. 18.

By reviewing the biovolume measurement approaches proposed in Sec. 3, DIP techniques are commonly applied in image pre-processing and segmentation tasks. The outcomes of different approaches can be evaluated systematically, which can be further used to analyze the measurement performance quantitatively. Moreover, with the development of deep learning, we found that there is no existing work on the deep learning-based biovolume measurement method. Hence several deep learning image segmentation methods are also applied for biovolume measurement and compared with classical segmentation methods.

This section is organized as follows: In Sect. 4.1, several image pre-processing methods, such as filtering and morphological operations, are compared. In Sect. 4.2, several segmentation approaches, which contain classical segmentation and deep learning based segmentation, are applied and evaluated to show their performance in the task of biovolume measurement.

4.1 Quantitative Analysis of Pre-processing Methods

Digital Image pre-processing methods are applied to deal with the noise and enhance the contrast. Gaussian filter is one of the linear filters, which can effectively suppress noise and smooth the image [81, 100]. The process of the Gaussian filter is similar to the mean filter. It takes the mean value of pixels in the filter window as the output. The mean filter window value is 1, but the value of the Gaussian filter decreases with the increase of distance from the center of the window. Therefore, the Gaussian filter performs less fuzzy to the image than a mean filter. Another widely applied filter is the median filter, which replaces the value of the center pixel as the median value of the sorted pixel in the filter window [62, 82, 89].

To show the denoising abilities of three filters above, the salt and pepper noise with a ratio of 0.3 and Gaussian noise with a mean of 0 and a variance of 0.01 are added to the images, respectively. Then, the images are denoised with three filters above. The images after filtering with 3×3 mean filter, 3×3 median filter and Gaussian filter with the cut-off frequency of 50 are shown in Fig. 19. Moreover, mean square error (MSE) and signal noise ratio (SNR) [116] are applied to evaluate the performance of denoising, which is shown in Table 4.

Table 3 Summary of image analysis based biovolume measurement for other microorganisms

Related work	Microorganism	Pre-processing methods	Segmentation methods
[18]	Fungi	Image enhancement and thinning operation	Thresholding
[87]	Alga		Thresholding
[92]	Alga	Neighborhood-averaging filter	
[88]	Fungi	Contour enhancement	Thresholding
[89]	Plankton	Median filter and local adaptive background correction	Thresholding
[95]	Plankton		Higher order local autocorrelational masks
[97]	Cyanobacteria		Thresholding
[86]	Phytoplankton	Equalize/Best fit	Thresholding
[90]	Cyanobacteria	High-pass filter and holes filling	Thresholding
[96]	Fungi	Roundness filter, width filter and height filter	Thresholding
[91]	ALga		Weighted RGB channels
[93]	Plankton		SVM
[98]	Waste water microorganisms	Debris elimination	Thresholding
[94]	Cyanobacteria	Adaptive brightness and contrast adjustment, Sobel operation and roundness filter	Random forest
[99]	Zooplankton		NIH-Image 1.62
[100]	Fungi	Median and high-pass Gauss filter	MicroImage 4.0
[101]	Fungi	High pass filter	KS400 software
[102]	Fungi	High-pass filter and a fixed threshold	KS400 software
[103]	Cyanobacteria		ImageJ v1.33f
[104]	Fungi	High-pass filter	ImageJ v1.33f
[105]	Cyanobacteria		ImageJ v1.37v
[106]	Microorganisms	Morphological operations	LUCIA G/F
[107]	Alga	Thresholding	Scion Image 4.0.2
[108]	Zooplankton		ZooScan Integrated System
[109]	Phytoplankton		AutoCAD
[110]	Phytoplankton		Opera Phenix
[111]	Algae		Blender 2.79 and NeuroMorph software
[112]	Mycoplasma	Median filter	Thresholding, Minitab and Amira
[113]	Cyanobacterial		NeuroMorf software

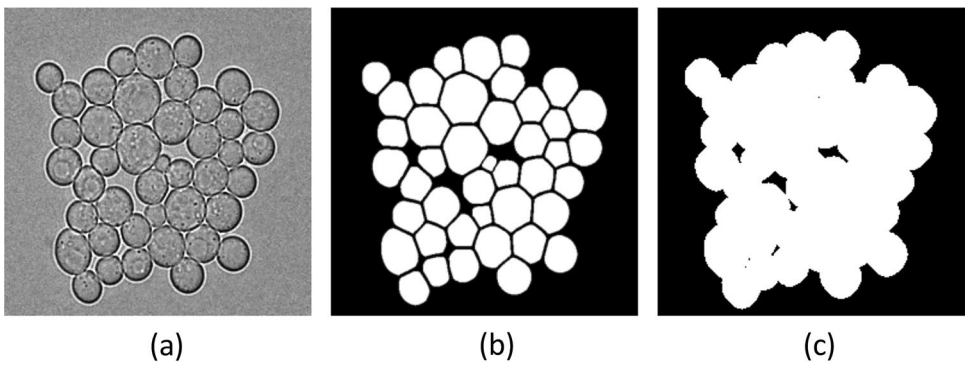

Fig. 18 **a** The original image; **b** The original mask; **c** Modified mask

By comparing the denoising results, the images after Median filtering have lowest MSE and highest SNR in both cases, indicating the process of Median filtering can maintain more information and suppress more noises. However, the results after Mean filtering and Gauss filtering seem unsatisfactory because of noises and blur contours, and showed low contrast between the objects and background.

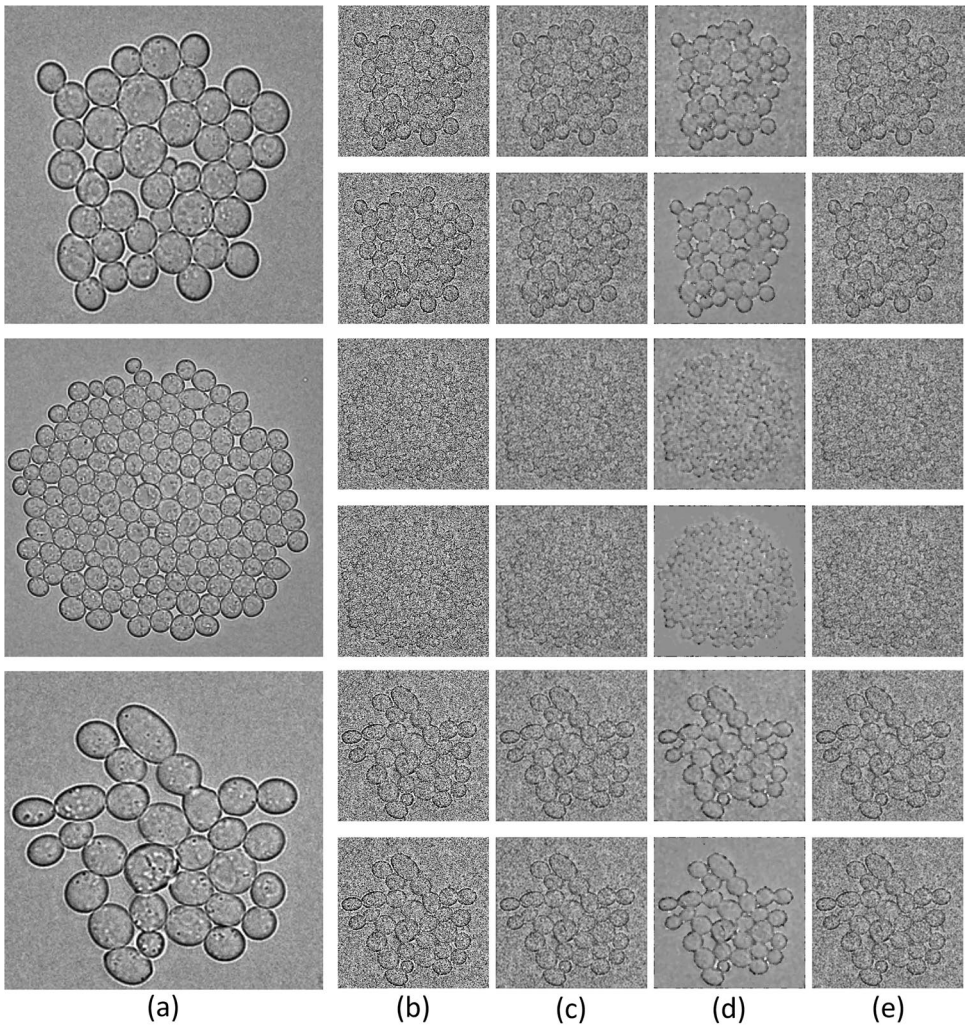

Fig. 19 **a** Original images; **b** Images after adding noises (upper for salt and pepper noise and below for Gaussian noise); **c** Images after mean filtering (upper for salt and pepper noise and below for Gaussian noise); **d** Images after median filtering (upper for salt and pepper noise and below for Gaussian noise); **e** Images after Gaussian filtering (upper for salt and pepper noise and below for Gaussian noise)

Table 4 The MSE and SNR (in dB) of denoised images based on three filters

Noise	Filters	MSE	SNR
Salt and pepper	Mean filter	110.56	27.71
	Median filter	**83.98**	**28.90**
	Gauss filter	106.72	27.86
Gaussian	Mean filter	110.42	27.71
	Median filter	**73.11**	**29.52**
	Gauss filter	106.06	27.89

The bold part represents the best value of each category. For Salt & Pepper nosie, the results processed by Median filter has the lowest MSE and the highest SNR, which is the best. For Gaussian noise, the Median filter also performs best

Morphological close operation can also be applied for denoising and debris erasing [94, 103]. The particles smaller than the size of kernel can be eliminated after close operation. The yeast images after close operation are shown in Fig. 20. The noise of images are apparently reduced, but the contours of yeast cells are relatively fuzzy.

Histogram equalization is one of the most used approaches for image enhancement [62, 63]. It stretches the histogram of the images as an approximately uniform distribution to enhance the contrast of the images. Histogram equalization can make the brightness distributes better on the histogram. It can enhance the local contrast without affecting the overall contrast, and histogram equalization achieve this function by effectively extending the commonly used brightness. The yeast images after global histogram equalization are shown in Fig. 21. The result is unsatisfactory because the noises spread all around the image, which makes the computer challenging to focus on the foreground and the background.

4.2 Quantitative Analysis of Segmentation Methods

In the task of image analysis based microorganism biovolume measurement, the segmentation performance

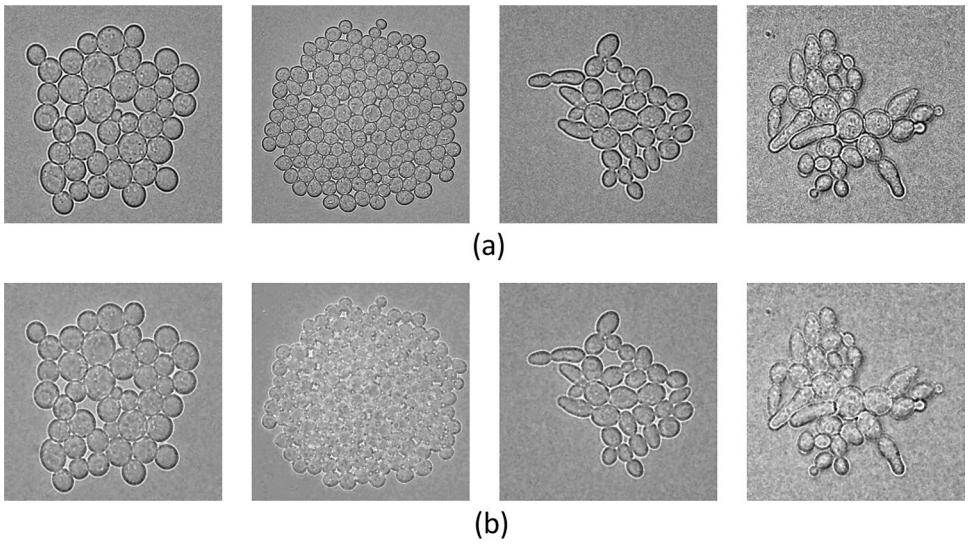

Fig. 20 **a** Original images; **b** Images after close operation

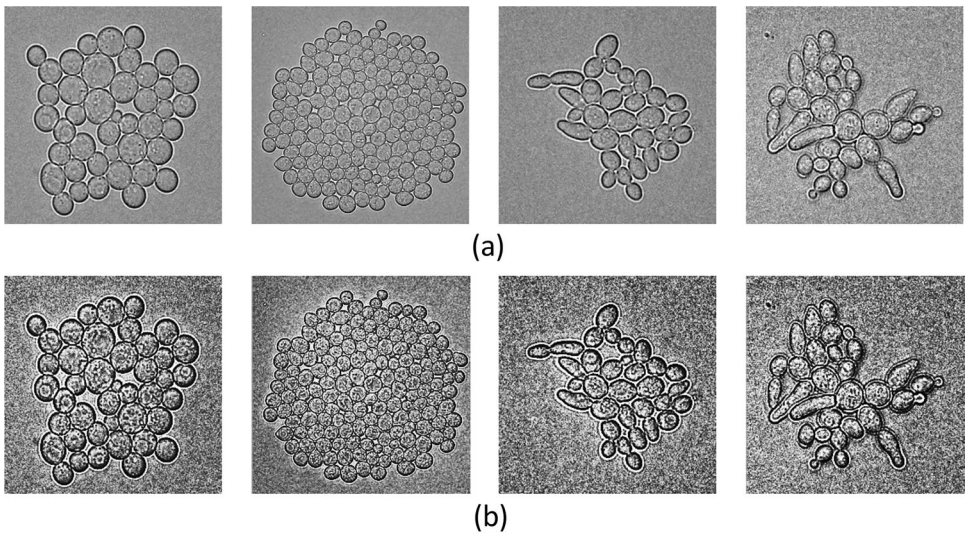

Fig. 21 **a** Original images; **b** Images after histogram equalization

determines whether the measurement result is good or not. The approaches based on thresholding can perform well when the foreground and background are in different range of gray scale, and they can easily be applied due to the small computation cost. The comparative results of thresholding (value=115) and Otsu Thresholding are shown in Fig. 22. It can be seen that both results have satisfactory segmentation performance, but the results after thresholding have more noise than the Otsu Thresholding results obviously, which need to be post-processed.

By reviewing the works of biovolume measurement, edge detection approaches are also widely applied [73, 94, 106]. The core algorithm of edge detection is to determine the edge pixels in the image first rather than connect these pixels to form the region boundary. Sobel operator is a discrete differentiation operator, which can be applied to calculate the approximate gradient of the grayscale image [94]. The pixel with a large gradient is more likely to be the edge. The Sobel operator can calculate the derivative in the horizontal and vertical directions, but it is relatively sensitive to the noise. Hence, the pre-processing of denoising is necessary. The canny operator is a multi-level detection algorithm that contains denoising, gradient calculation, non-maximal suppression, and the method of double thresholding [117]. Non-maximum suppression is an edge thinning method to retain the local maximum gradients and suppress the other gradients. The canny operator performs well for most of the images. In the Marr-Hildreth operator, a Gaussian filter is applied first for smoothing, and then the Laplacian is applied for image enhancement [73]. Finally, the point of intersection between zero axis and the second derivative line can be determined as the edge. The comparative results of Sobel, Canny and Marr-Hildreth are shown in Fig. 23. The segmentation results of Sobel operator have more noise

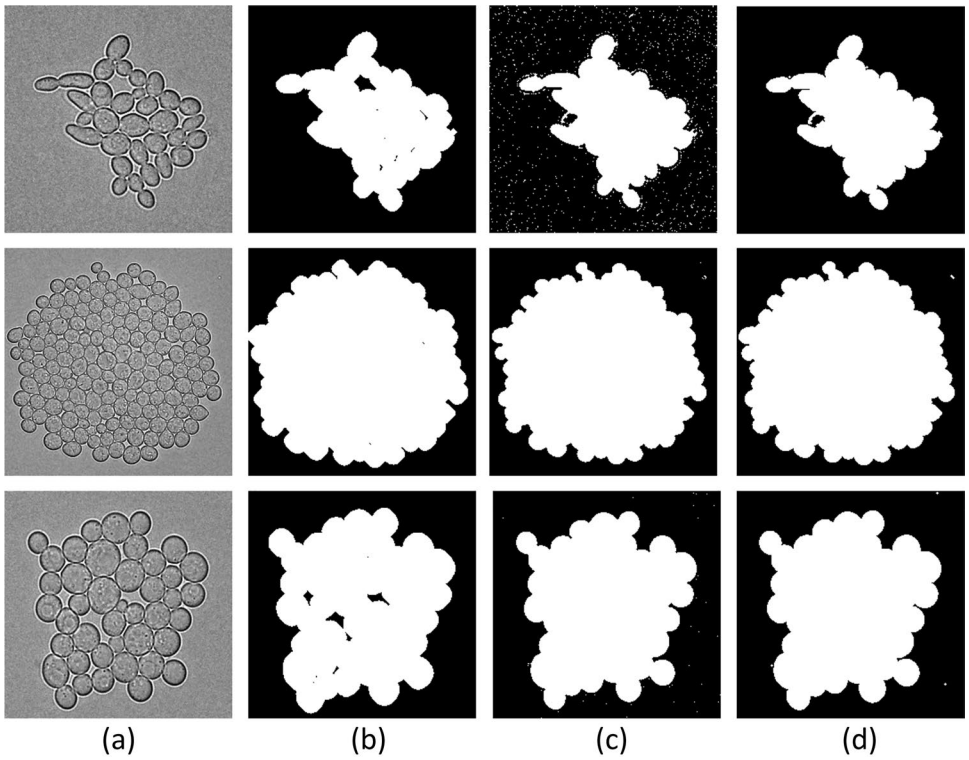

Fig. 22 **a** Original images; **b** Ground truth; **c** Thresholding based segmentation (value = 115); **d** Otsu Thresholding based segmentation

obviously, and the Marr-Hildreth results have the problem of over-detection, which means many inner pixels are classified as edge. Canny operator performs best by comparing with the other approaches.

Watershed is a segmentation method based on region growing [104]. The gray level of all pixels are sorted and then the growing region is labelled based on local minimum. The results of watershed is shown in Fig. 24. It can be seen that the watershed approach has the problem of over-segmentation,hence it may meet the requirements of adherent objects separation, but should not be applied for global segmentation.

Since the development of deep learning, several excellent backbones (such as SegNet and U-Net) have been widely applied for image segmentation and can obtain satisfactory results [118, 119]. The first 13-layer convolutional networks of VGG16 are applied in SegNet as an encoder, and SoftMax is applied for classification after the decoder. U-Net is an end-to-end net of image segmentation with an encoder and a decoder. It was designed for medical image segmentation, which meets the similar requirements of biovolume measurement as both of them are microscopic images, and the datasets are limited. SegNet and U-Net train the yeast dataset for 60 epochs with a batch size of 8. The CNN-based models can be trained independently without relying on feature engineering, and the models can obtain the expected results, showing strong generalization abilities. The most-used pre-processing approach in deep learning is data augmentation to avoid overfitting and to increase generalization capabilities, but a limited pre-processing technique is used for denoising [120]. Here, SegNet and U-Net are end-to-end models trained without any pre-processing or pre-training. The segmentation results of SegNet and U-Net are shown in Fig. 25. The results show that U-Net has better performance for biovolume measurement, which means that concatenated operation of encoder and decoder can improve the precision of segmentation.

To quantitative analyze the performance of segmentation approaches above, several classical indices are applied for evaluation, including Accuracy, Dice, Jaccard, Precision and Hausdorff distance. The definition of Accuracy, Dice, Jaccard (IoU) and Precision are summarized in Table 1. Hausdorff distance is applied to measure the Euclidean distance between the predicted and GT images [121]. Dice is more sensitive to the inner filling of the mask, while Hausdorff Distance is more sensitive to the separated boundary. The comparative results of different approaches is shown in Table 5.

It is observed that the segmentation performance of deep learning models are much more better than the classical segmentation approaches, obviously. Canny operator achieves the best result in classical segmentation methods, which is much more better than Sobel and Marr-Hildreth operators. U-Net is the best model in the task of microorganism biovolume measurement, indicating that the architecture of

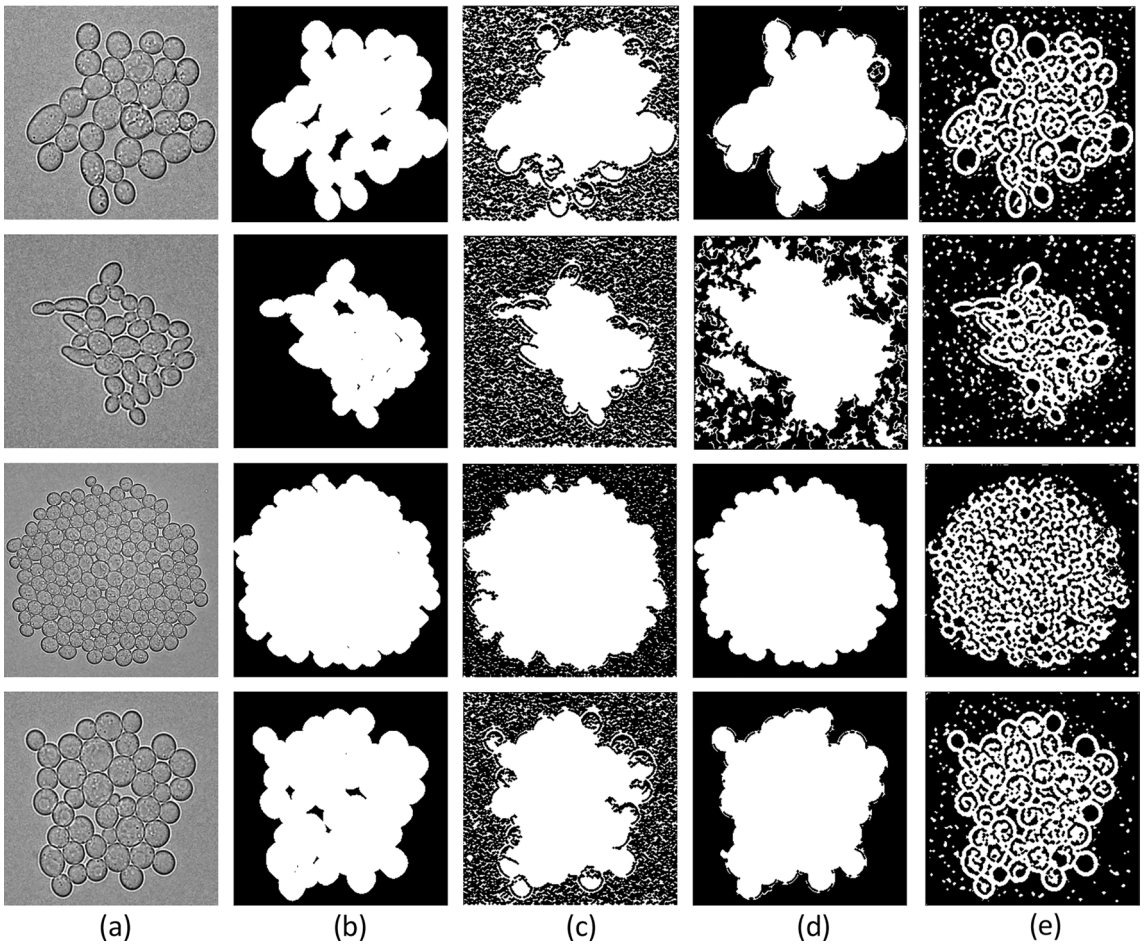

Fig. 23 **a** Original images; **b** Ground truth; **c** Sobel operator based segmentation; **d** Canny operator based segmentation; **e** Marr-Hildreth operator based segmentation

encoder-to-decoder and concatenation operation can indeed improve the capability of image segmentation.

5 Measurement Methods Analysis and Discussion

The microorganism biovolume measurement methods based on DIP are summarized in Sect. 3. By reviewing all the approaches, image pre-processing and segmentation are the most import tasks in biovolume measurement. The performances of these methods are summarized and analyzed, including their advantages and potential applications.

5.1 Image Pre-processing Methods

Most microorganisms are mirrored as colorless and have the same color as the environment. So, the color feature is not worthy of image segmentation. Moreover, due to the inhomogeneity of the illumination and imaging noise, pre-processing approaches can be used for denoising and contrast enhancement.

At first, the images are converted to gray-level images to eliminate the worthless color feature. After that, the Intensity of images with Hue-Saturation-Intensity (HSI) can be changed individually, that has no influence to color of images, such as the works in [91], [100].

Secondly, the Gaussian low-pass filter and linear transformation can be applied to reduce the influence of uneven illumination, which is caused by uneven shading, such as the work in [103].

Thirdly, denoising is necessary for preparation of subsequent image segmentation. The median filter and Gaussian filter perform well for noise removal, which are widely applied. Gaussian filter is a linear smoothing filter to eliminate Gaussian noise, which is widely applied in image denoising. Gaussian filtering denoising is the weighted average of the gray value of the whole image. The value of each pixel is calculated by the weighted average of its own value and the value of the neighbor pixels. Median filter is

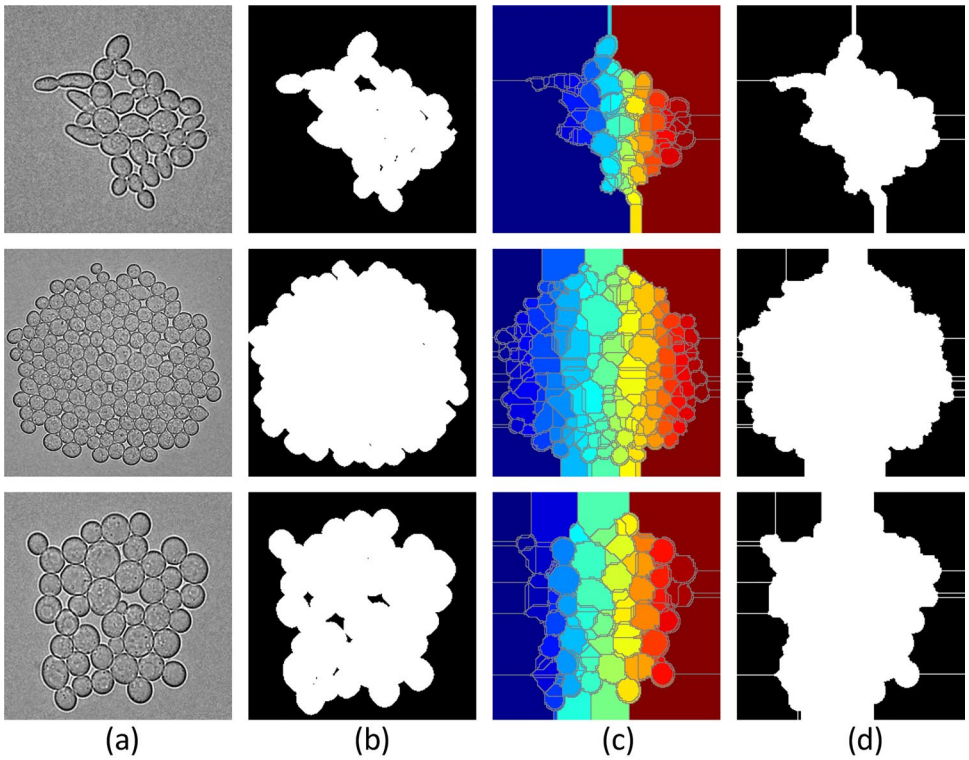

Fig. 24 **a** Original image; **b** Ground truth; **c** Watershed based segmentation of each region; **d** Watershed based segmentation for foreground and background

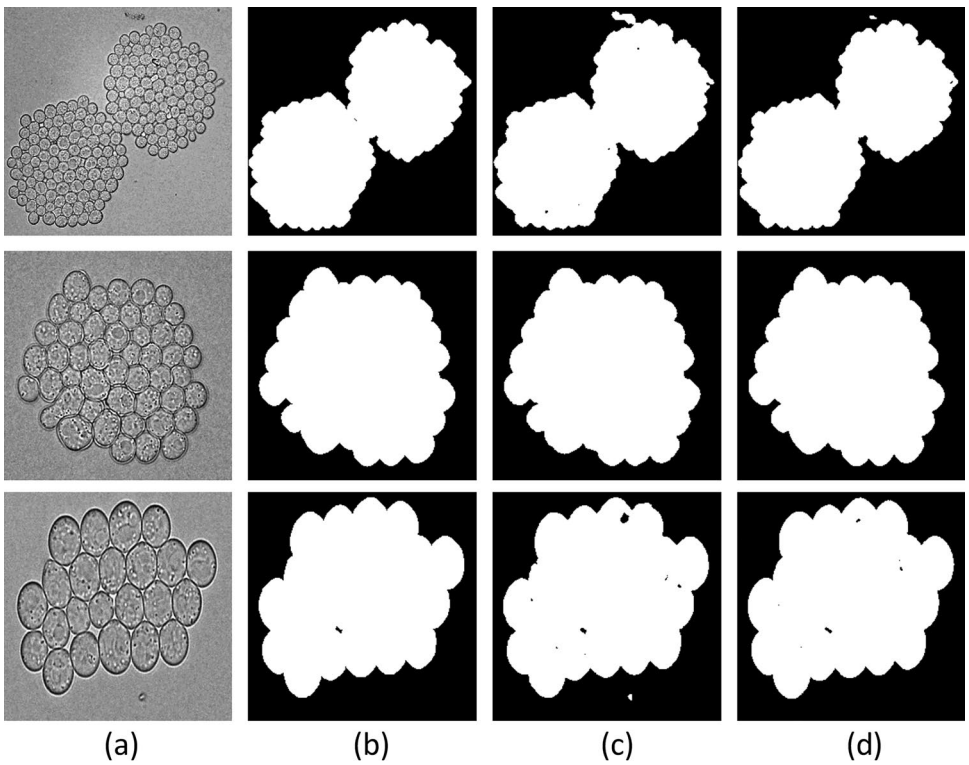

Fig. 25 **a** Oiginal images; **b** Ground truth; **c** SegNet segmentation; **d** U-Net segmentation

a non-linear smoothing filter, which replaces the gray value of the pixel as the median gray value of neighbor pixels. The comparison of Gaussian filter and Median filter is illustrated in Fig. 19, which shows the Gaussian filter with proper parameters performs best in the task of image denoising. The application of morphological close operation can remove

Table 5 The average segmentation evaluation indices of predicted images

Methods	A	D	J	P	H
Thresholding	92.31	87.67	80.83	93.05	6.14
Otsu	90.24	89.35	83.73	90.47	5.91
Sobel	76.34	76.55	64.43	70.21	10.31
Canny	91.22	90.03	84.69	88.95	5.90
Marr-Hildreth	72.17	63.71	47.49	78.07	10.11
Watershed	88.09	85.86	76.68	84.12	8.21
SegNet	98.64	**98.51**	97.10	99.31	3.77
U-Net	**98.97**	98.43	**97.11**	**99.61**	**3.39**

The bold part represents the best value of each column, which shows the U-Net has the best performance for microorganism biovolume measurement except DIce

the useless debris. The performance of close operation is shown in Fig. 20, the noise of image is erased and the contour lines are smoothed, but the edges are relatively fuzzy, which makes it difficult for segmentation. High-pass filter can also be used for denoising, such as the work in [102], the performance is shown in Fig. 26.

Finally, the colorless microorganisms have low contrast resolution, which are inconspicuous in environment. Contours with high contrast can perform better in image segmentation. One of the most frequently-used global methods is gray level histogram equalization, which has satisfactory result in most images, such as the work in [63]. Histogram equalization can indeed improve the contrast of the foreground and the background, which is shown in Fig. 20. It shows that the contour lines of yeast cells are enhanced and easy to identify, which is helpful for image segmentation. However, the image noises in the background are enhanced meanwhile, hence the denoising operation is necessary to reduce the influence of noises. In [94], contours closing, holes filling and Sobel operation are applied to make solid and unambiguous areas for contour enhancement, the performance is shown in Fig. 27.

5.2 Image Segmentation Methods

Image segmentation is the most vital task in microorganism biovolume measurement. The colony region needs to be segmented from the whole image for subsequent processing.

At first, thresholding based image segmentation methods are widely used for microorganism biovolume measurement. Global thresholding can easily segment the regions of colony after proper pre-processing, such as the works in [66]. The results of global thresholding on a benchmark dataset are shown in Fig. 22. By comparing with the ground truth, the contour lines of yeast cells are segmented precisely, but some inner holes are wrongly classified as the foreground. Hence, the global thresholding can obtain the satisfactory

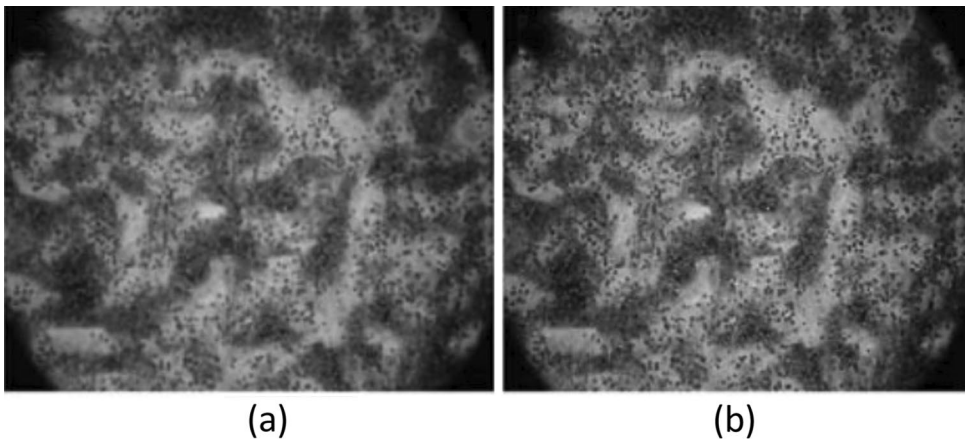

Fig. 26 **a** The original image; **b** The image after high pass filtering (In [102] Fig. 1)

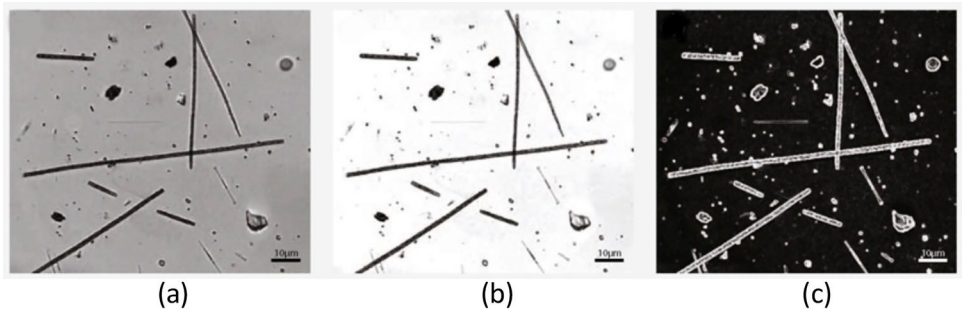

Fig. 27 **a** The original image; **b** The image after contrast enhancement; (c) The image after using Sobel filter (In [94] Fig. 1)

segmentation results in general, but there are still some problems in detail.

Secondly, the performance of Otsu Thresholding, such as the works in [67], [68] and [81], seems more satisfactory with fast computing speed. However, the process of noise removal is necessary before Otsu Thresholding calculation because of the high sensitivity. The performance of Otsu Thresholding based image segmentation is shown in Fig. 28. The results of Otsu Thresholding on a benchmark dataset are shown in Fig. 22. By comparing with the segmentation results of global thresholding, Otsu Thresholding based segmentation have less noise and the result is more similar to the ground truth, which is proved in Table. 5, that is, he Hausdorff distance of Otsu Thresholding based segmentation result is less than the result obtained by global thresholding.

Thirdly, the approaches of edge detection are widely spread in microorganism biovolume measurement. Sobel edge detection method performs well in microorganism segmentation, such as the work in [94]. The combination method of Gaussian filter and Laplacian filter, that is, Marr-Hildreth operator, performs well for image denoising and contour enhancement, such as the work in [73]. In [106], a Mexican hat filter is applied for edge detection, which is the second derivative of the Gauss function. The advantage of the Mexican Hat wavelet transform is that it has good localization in the time domain and frequency domain. It is symmetric and can be used for the continuous wavelet transform. And it is close to the spatial response characteristics of human eyes. The comparison results based on the proposed edge detection approaches on a benchmark dataset are shown in Fig. 23. It shows that Sobel operator based edge detection is sensitive to noises, which means lots of noises of the background are recognized as the foreground. Hence the denoising operation is necessary before Sobel filtering. The segmentation results of Marr-Hildreth operator exist the problem of over-segmentation. Many inner pixels are identified as the edge and the results remain a lot of noises. Canny operator based segmentation performs best, most of the noises are erased and the contour lines are relatively clear and accurate. The quantitative analysis in Table. 5 also proves that Canny operator based segmentation has the highest accuracy and the lowest Hausdorff distance, which shows it has the highest similarity with ground truth.

Finally, the adherent colonies need to be separated, which is usually achieved by using watershed algorithm. Separation of attached colonies is necessary when the biovolume need to be calculated individually, such as the work in [104]. The segmentation results based on watershed is shown in Fig. 24. Watershed can segment the images into several individual parts and the contour lines can be detected accurately, indicating it can perform well in the task of microorganism counting (meet the requirement of separate the clustered colony into individual cells). However, the problems of over-segmentation still need to be solved.

5.3 Image Post-Processing Methods

Classification is necessary when measuring the biovolume of microorganisms. According to supervised learning, the

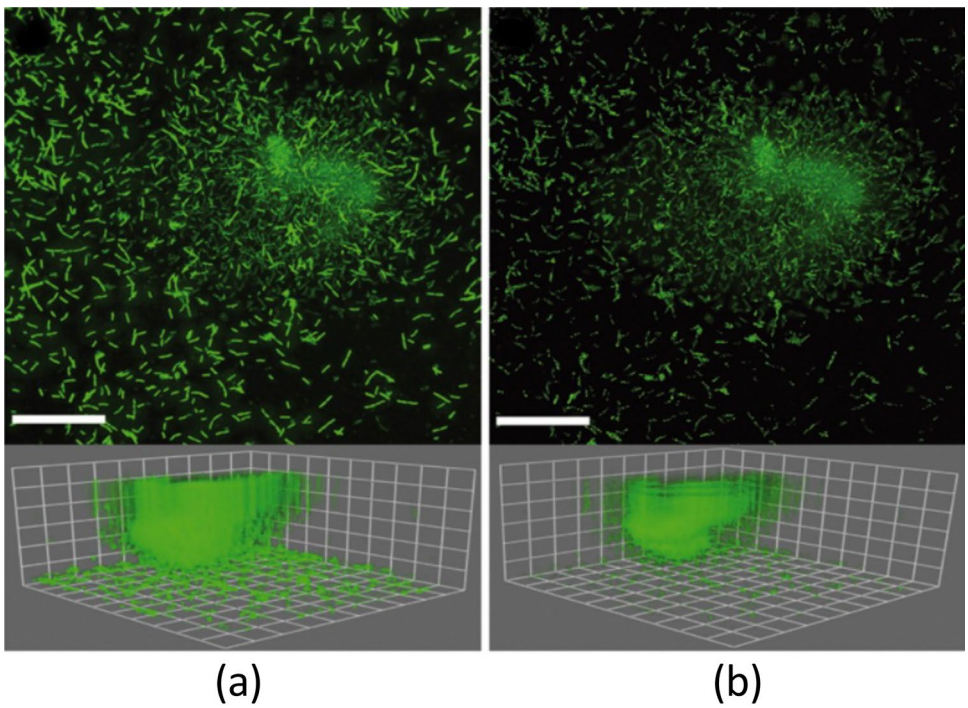

Fig. 28 **a** The original image; **b** The image after Otsu Thresholding (In [68] Fig. 2)

support vector machine (SVM) is one of the classical linear classifiers, such as the work in [93]. The morphological features are obtained for training, and the classification groups are shown in Fig. 29. SVM performs well with small samples and can be applied for high-dimensional classification using different kernels.

Secondly, an artificial neural network (ANN) is a self-learning non-linear network with strong fault tolerance. In [92], an ANN is used to relate the cell density in the photobioreactor with the digitized images. ANN can learn the classification mechanism automatically, which can be applied to obtain the satisfactory results, but the learning process is unobservable and the output is hard to interpret.

Thirdly, roundness filter is applied to remove useless debris after segmentation, such as the work in [96]. In [94], the roundness value of remaining elements is estimated to erase all objects with a roundness value> 0.4. When the target particles are circular, the particles with low roundness value should be erased. However, when the target particles are non-circular, such as fungi and alga, the particles with high roundness value should be erased. The performance is shown in Fig. 30.

5.4 Analysis of Potential Methods

The microorganism biovolume measurement approaches based on DIP can not only be referred by microbial measurement researches, but also referred by other DIP fields. For example, such as the environmental microorganism classification [122–125], blood cell classification [126], classification for different types of microorganisms [38, 122, 127], microorganism image generation [128], microorganism

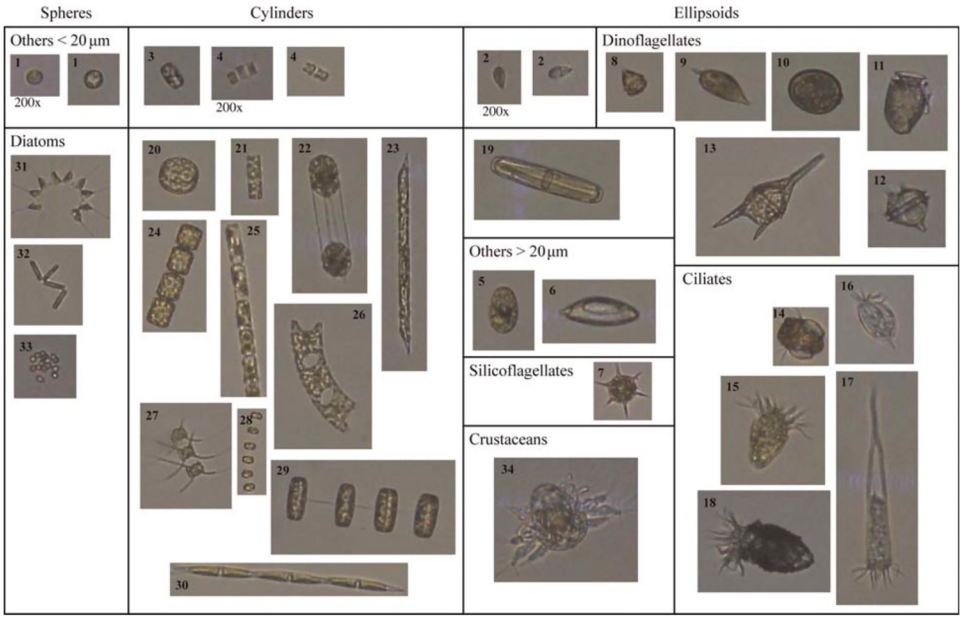

Fig. 29 The classification groups with their morphological features (In [93] Fig. 2)

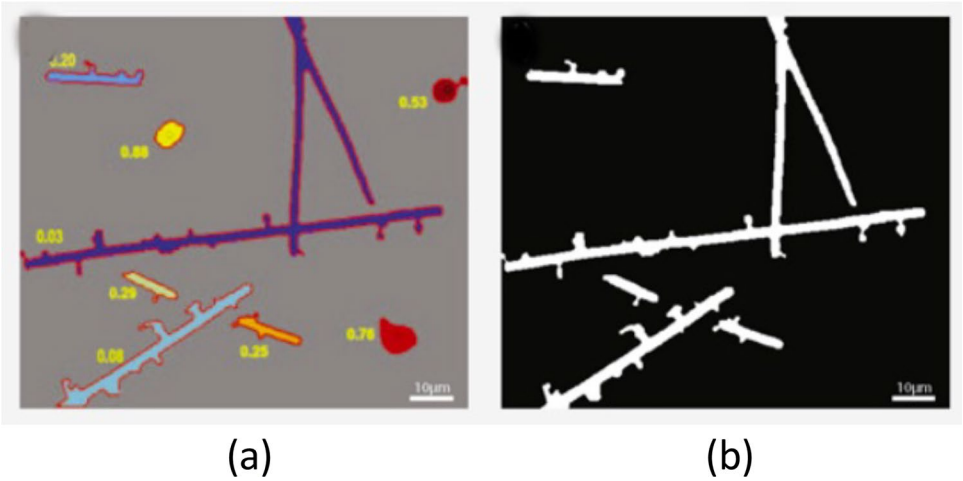

Fig. 30 **a** Roundness calculation; **b** The round particles are removed using thrsholding (In [94] Fig. 2)

object detection [129], medical image classification [130, 131], medical object tracking [132, 133] and human health monitoring [134–136]. After that, the segmentation methods for microorganisms can be referred to by DIP researchers, such as stem cell segmentation [137], near-duplicate detection [138], image enhancement [139], cancer cell segmentation [140], and environmental microorganism segmentation [118, 141, 142]. Moreover, microscopic image processing performs an essential role in industrial analysis, such as the monitoring for wastewater [143], beef carcass evaluation [144], monitoring of bacteria in milk [145], monitoring flames in an industrial boiler [146], softwood lumber grading [147] and so on.

Microorganism quantification consists of microorganism biovolume measurement and microorganism colony counting, and the colony counting can be regarded as a measurement approach with higher accuracy. Object counting is one of the most essential parts of computer vision, which can be modified and applied in microorganism quantification.

In [148], the reverse perspective network is applied for object counting to solve the problem of input image scale variation. The perspective estimator can calculate the perspective parameter and the coordinate transformer can convert the images to similar size. The weight of ground truth is promoted for training by using an adversarial network. The proposed method can obtain the satisfactory result for the dataset with large variation of scale. The frame work of proposed method is shown in Fig. 31.

In [149], the traditional detection based methods are replaced by the density estimation based crowd counting methods, which can detect the density of crowd with high performance and high precision. However, the encoder and decoder of traditional CNN based density estimation methods have low correlation, which is difficult to remain the spatial information of the image. The Trellis Encoder-Decoder networks including multi-path decoder and encoder, is proposed to improve the accuracy of counting. The structure of network is shown in Fig. 32. Only two pooling layers are applied to reduce the loss of spatial pixel accuracy. In addition, a multi-scale encoder is designed to improve the adaptability of network to the large variation of the object size.

In [150], an image-leve supervision based image segmentation method is proposed for object counting. The traditional object counting approaches based on regression can obtain the counting results with high accuracy. However, the results can only reflect the global counting but cannot locate the objects that are counted. The Image-level lower-count (ILC) supervised density map estimation is proposed in this article for crowd counting and segmentation. The architecture of the network is shown in Fig. 33.

In addition, the development of an attention mechanism can be applied in image processing to focus on the region of interest (ROI). Spatial transformer networks (STN) can locate the region of interest and transform it into an ideal image by affine transformation, and then put it into the neural network for training [151]. STN consists of Localisation net, Grid generator and Sampler. The Localisation net can be applied for calculation of affine transformation parameters. The Grid generator can find the mapping between output and input features, and the corresponding relation of pixel coordinates is obtained. The Sampler can select input features based on the position mapping and transformation parameters, and output the image with bilinear interpolation. The architecture of STN is shown in Fig. 34.

Another network based on attention mechanism is Squeeze-and-Excitation Networks (SENET). The application of attention mechanism in STN is based on the spatial domain, while SENET is based on the channel domain. SENET can learn the correlation of each feature channel, and the weight value of each channel is calculated, so that the following network can improve the selected significant feature channels and the unworthy feature channels are restrained. The structure of SENET is shown in Fig. 35. The satisfactory ROI extraction method provided by the

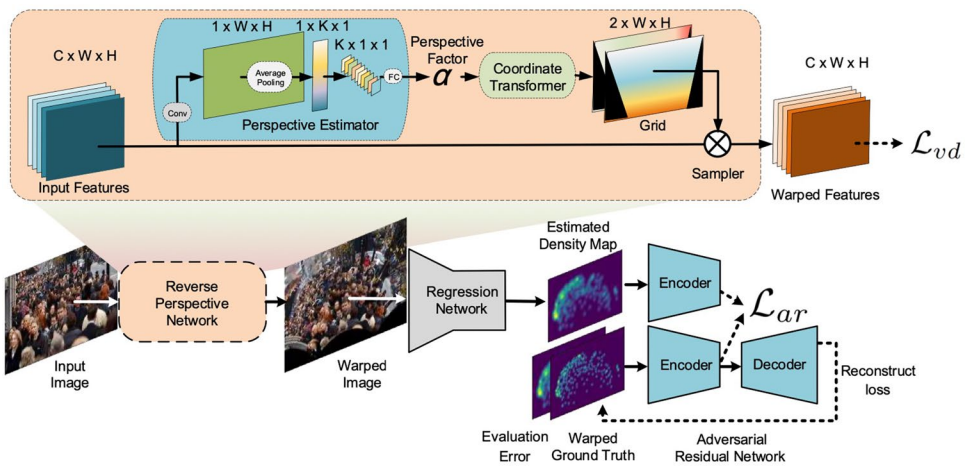

Fig. 31 The framework of reverse perspective network (In [148] Fig. 4)

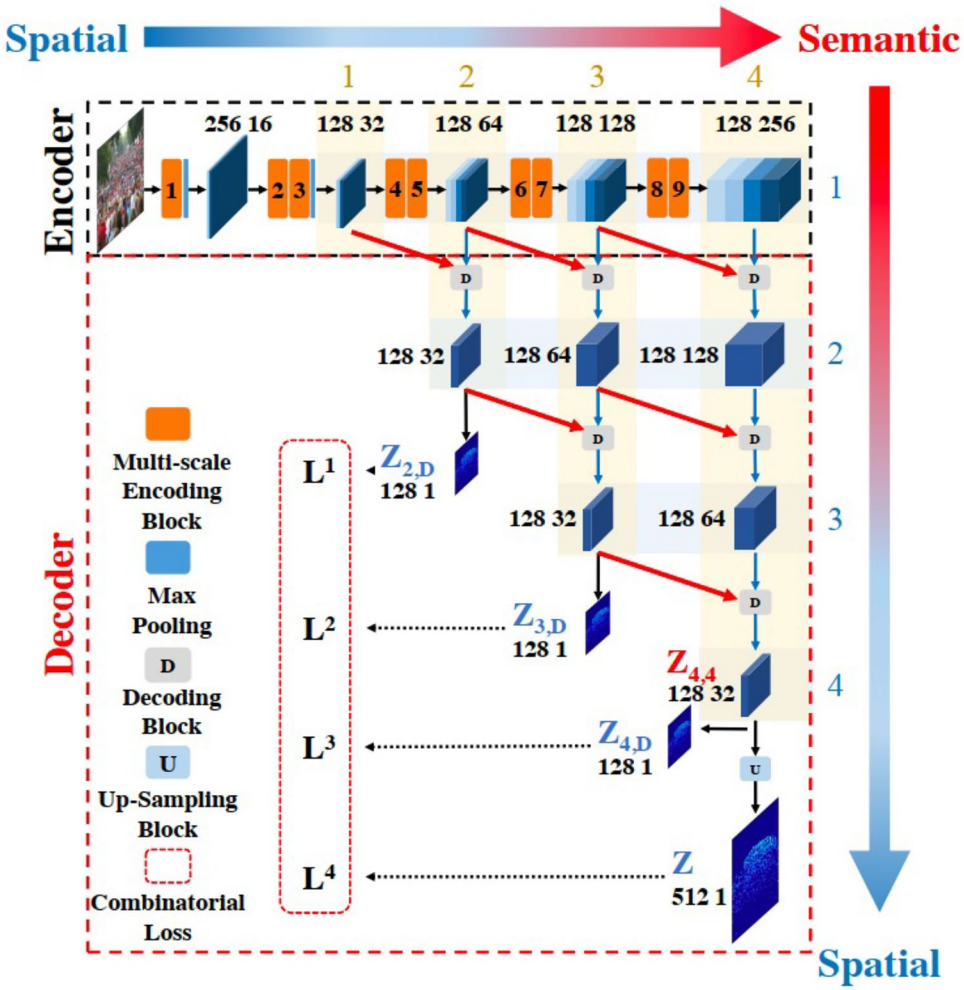

Fig. 32 The architecture of Trellis Encoder-Decoder network (In [149] Fig. 1)

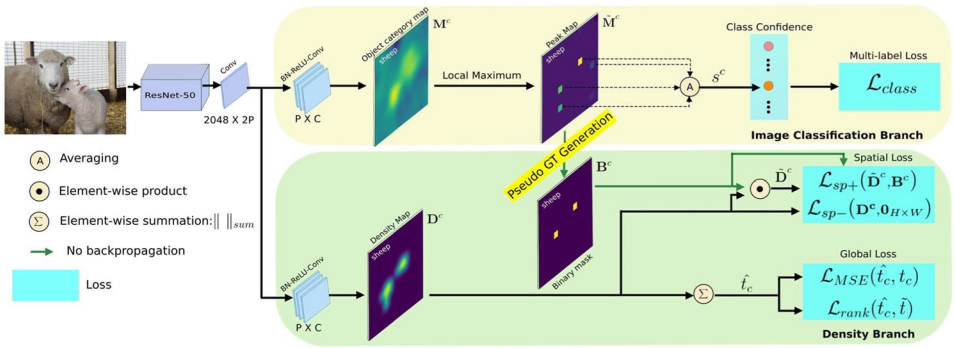

Fig. 33 The architecture of object counting method (In [150] Fig. 3)

attention mechanism can support a possibility to extract the target microorganism region in an image with a complex environment.

Furthermore, Transformer is a type of self-attention mechanism-based deep neural network that is wildly used in natural language processing (NLP). A transformer has been developed to satisfy computer vision because of the strong representation ability recently. The use of Transformer performs better by comparing with other networks, such as CNN, which has shown strong competitiveness [153]. A transformer has a more robust ability of global information representation than CNNs, making it possible to describe the microorganism structure in a complete image. Especially, Vision Transform (ViT) is one of the most remarkable visual transformer method till now, which directly applies sequences of image patches (with

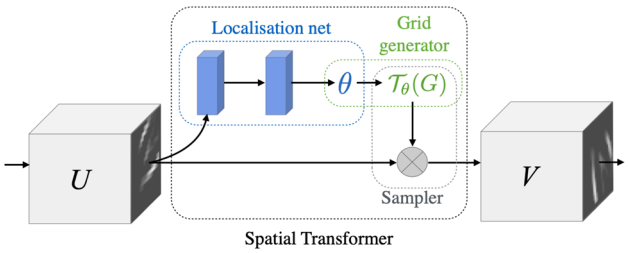

Fig. 34 The structure of a spatial transformer module (In [151] Fig. 2)

position information) as input first. The ViT projects the patches to the original transformer encoder and classifies the images with a multi-head attention mechanism as it does in NLP tasks. The framework of ViT is shown in Fig. 36.

Finally, the development of microorganism biovolume measurement based on DIP has high correlation with the development of relevant researches, such as the technique of immunofluorescence staining for cells [155], confocal laser scanning microscope (CLSM) imaging [156], epifluorescence microscope equipment [157], and so on.

6 Conclusion

In this paper, a comprehensive review of DIP based microorganism biovolume measurement is proposed. The current methods are generalized and summarized, and grouped as bacteria and other microorganisms, such as fungi, alga and so on. In each type of microorganism summarization, the methods are grouped based on image segmentation algorithm, including classical thresholding methods, self-designed methods, and third-party tools. In Sects. 3.1.1 and 3.2.1, it can be seen that the classical approaches are developed first, from 1980s to 2000s. By reviewing the classical methods, the performances are limited and unsatisfied. In Sects. 3.1.1 and 3.2.1, the development of self-designed methods for biovolume measurement is rapid. Self-designed methods can process the microorganism data by using specific approaches to match their different features, which show satisfactory result by comparing with the classical methods. In Sect. 3.1.3 and Sect. 3.2.3, a mass of professional DIP systems are applied for microorganism biovolume measurement, such as 'ImageJ' and 'CellC'. The integration software are more professional and performs well in specific field of biovolume measurement, which shows the microorganism biovolume measurement is increasing important. In conclusion, the prosperous development of DIP based microorganism biovolume measurement methods show

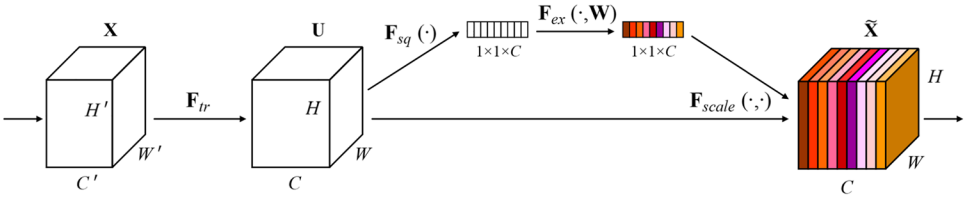

Fig. 35 The structure of one Squeeze-and-Excitation block in SENET (In [152] Fig. 1)

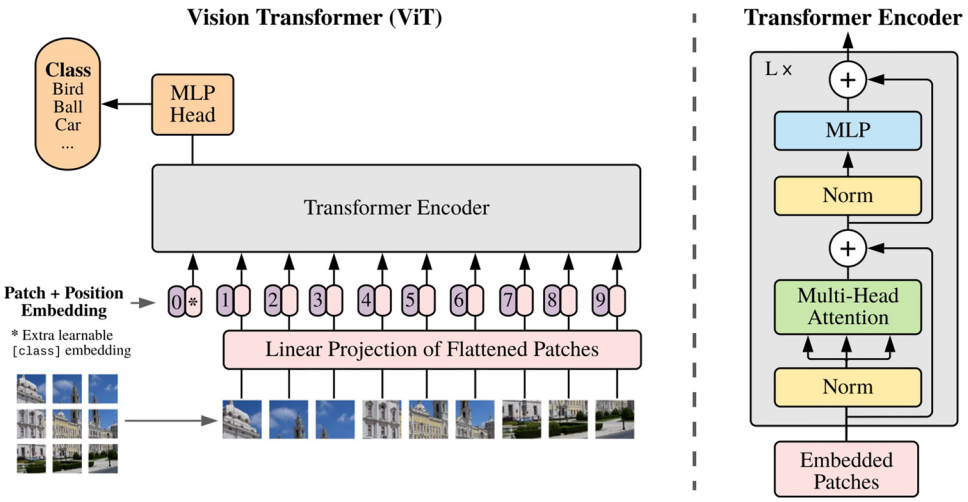

Fig. 36 The structure of the ViT (In [154] Fig. 1)

the extensive research potential in microbial research. After that, in Sect. 4, the most used image pre-processing and segmentation approaches are quantitatively analyzed to show their performance in the task of microorganism biovolume measurement. Finally, the widely applied microorganism biovolume measurement approaches such as image pre-processing, image segmentation, and connected domain detection are analyzed in Sect. 5.

Acknowledgements This work is supported by the "Natural Science Foundation of China" (No. 61806047), "Sichuan Science and Technology Program" (No. 2021YFH0069, 2021YFQ0057, 2022YFS0565). We thank Miss Zixian Li and Mr. Guoxian Li for their important discussion.

References

1. Madigan MT, Martinko JM, Parker J et al (1997) Brock biology of microorganisms, vol 11. Prentice hall Upper Saddle River, NJ
2. Cui J, Li F, Shi ZL (2019) Origin and evolution of pathogenic coronaviruses. Nat Rev Microbiol 17(3):181–192
3. Andersen KG, Rambaut A, Lipkin WI, Holmes EC, Garry RF (2020) The proximal origin of SARS-CoV-2. Nat Med 26(4):450–452
4. Li, C., Zhang, J., Kulwa, F., Qi, S., Qi, Z.: A SARS-CoV-2 Microscopic Image Dataset with Ground Truth Images and Visual Features. In: Chinese Conference on Pattern Recognition and Computer Vision (PRCV). pp. 244–255. Springer (2020)
5. Webster J, Weber R (2007) Introduction to fungi. Cambridge University Press, Cambridge
6. Coutteau P (1996) Micro-algae. Manual on the production and use of live food for aquaculture 361:7–48
7. Hui DS, Azhar EI, Madani TA, Ntoumi F, Kock R, Dar O, Ippolito G, Mchugh TD, Memish ZA, Drosten C et al (2020) The continuing 2019-nCoV epidemic threat of novel coronaviruses to global health-The latest 2019 novel coronavirus outbreak in Wuhan China. Int J Infect Dis 91:264–266
8. Rahaman MM, Li C, Yao Y, Kulwa F, Rahman MA, Wang Q, Qi S, Kong F, Zhu X, Zhao X (2020) Identification of COVID-19 samples from chest X-Ray images using deep learning: a comparison of transfer learning approaches. J X-ray Sci Technol 28(5):821–839
9. University, J.H.: Coronavirus covid-19 global cases by the center for systems science and engineering (csse) at johns hopkins university (jhu). Available at: https://coronavirus.jhu.edu/map.html (2020)
10. Liu X, Wang S, Sendi L, Caulfield MJ (2004) High-throughput imaging of bacterial colonies grown on filter plates with application to serum bactericidal assays. J Immunol Method 292(1–2):187–193
11. Rajapaksha P, Elbourne A, Gangadoo S, Brown R, Cozzolino D, Chapman J (2019) A review of methods for the detection of pathogenic microorganisms. Analyst 144(2):396–411
12. Chien TI, Kao JT, Liu HL, Lin PC, Hong JS, Hsieh HP, Chien MJ (2007) Urine sediment examination: a comparison of automated urinalysis systems and manual microscopy. Clinica Chimica Acta 384(1–2):28–34
13. Thiran, J.P., Becks, M.O., Macq, B.M., Mairesse, J.: Automatic recognition of cancerous cells using mathematical morphology. In: Visualization in Biomedical Computing 1994. vol. 2359, pp. 392–401. International Society for Optics and Photonics (1994)
14. Zhang, J., Li, C., Grzegorzek, M.: Applications of Artificial Neural Networks in Microorganism Image Analysis: A Comprehensive Review from Conventional Multilayer Perceptron to Popular Convolutional Neural Network and Potential Visual Transformer. arXiv preprint arXiv:2108.00358 (2021)
15. Zhang J, Li C, Rahaman MM, Yao Y, Ma P, Zhang J, Zhao X, Jiang T, Grzegorzek M (2021) A comprehensive review of image analysis methods for microorganism counting: from classical image processing to deep learning approaches. Artificial Intel Rev 1:1–70
16. Gray A, Young D, Martin N, Glasbey C (2002) Cell identification and sizing using digital image analysis for estimation of cell biomass in High Rate Algal Ponds. J Appl Phycol 14(3):193–204
17. Rousso BZ, Bertone E, Stewart RA, Hughes SP, Hobson P, Hamilton DP (2022) Cyanobacteria species dominance and diversity in three Australian drinking water reservoirs. Hydrobiologia 849(6):1453–1469
18. Morgan P, Cooper C, Battersby N, Lee S, Lewis S, Machin T, Graham S, Watkinson R (1991) Automated image analyss method to determine fungal biomass in soils and on solid matrices. Soil Biol Biochem 23(7):609–616
19. Tucker KG, Kelly T, Delgrazia P, Thomas CR (1992) Fully-automatic measurement of mycelial morphology by image analysis. Biotechnol Prog 8(4):353–359
20. Gonzalez, R.C., Woods, R.E., Eddins, S.L.: Digital image processing using MATLAB. Pearson Education India (2004)
21. Amrita, Kaur L (2016) Image processing techniques on agriculture-A review. Research Cell: An Internat J Eng Sci 22:515–526
22. Sudiana D, Rizkinia M (2012) ALOS/PALSAR image processing using Dinsar and log ratio for flood early detection in Jakarta based on land subsidences. Makara J Technol 15(2):193–200
23. Pesatori, A., Magnani, A., Norgia, M.: Infrared image sensor for fire location. In: 2013 IEEE International Instrumentation and Measurement Technology Conference (I2MTC) (2013)
24. Ebrahimi, A., Amirkhani, A., A Raie, A., Mosavi, M.R.: Car license plate recognition using color features of Persian license plates. Journal of Advances in Computer Research **6**(4), 27–38 (2015)
25. Li, C., Chen, H., Li, X., Xu, N., Hu, Z., Xue, D., Qi, S., Ma, H., Zhang, L., Sun, H.: A review for cervical histopathology image analysis using machine vision approaches. Artificial Intelligence Review pp. 1–42 (2020)
26. Li, C., Li, X., Rahaman, M., Li, X., Sun, H., Zhang, H., Zhang, Y., Li, X., Wu, J., Yao, Y., et al.: A comprehensive review of computer-aided whole-slide image analysis: from datasets to feature extraction, segmentation, classification, and detection approaches. arXiv preprint arXiv:2102.10553 (2021)
27. Li, Y., Li, C., Li, X., Wang, K., Rahaman, M.M., Sun, C., Chen, H., Wu, X., Zhang, H., Wang, Q.: A comprehensive review of markov random field and conditional random field approaches in pathology image analysis. Archives of Computational Methods in Engineering pp. 1–31 (2021)
28. Zhou X, Li C, Rahaman MM, Yao Y, Ai S, Sun C, Wang Q, Zhang Y, Li M, Li X et al (2020) A comprehensive review for breast histopathology image analysis using classical and deep neural networks. IEEE Access 8:90931–90956
29. Liu W, Li C, Rahaman MM, Jiang T, Sun H, Wu X, Hu W, Chen H, Sun C, Yao Y et al (2022) Is the aspect ratio of cells important in deep learning? A robust comparison of deep learning methods for multi-scale cytopathology cell image classification: From convolutional neural networks to visual transformers. Comput Biol Med 141:105026
30. Ekstrom MP (2012) Digital image processing techniques, vol 2. Academic Press, New York

31. Qiu D, Jiao N, Qian L (2004) Advance in measured techniquesof aquatic bacterial counting and cell sizes. J Oceanography Taiwan Strait 23(3):376–385
32. Gracias KS, McKillip JL (2004) A review of conventional detection and enumeration methods for pathogenic bacteria in food. Canadian J Microbiol 50(11):883–890
33. Daims H, Wagner M (2007) Quantification of uncultured microorganisms by fluorescence microscopy and digital image analysis. Appl Microbiol Biotechnol 75(2):237–248
34. Dazzo FB, Niccum BC (2015) Use of CMEIAS image analysis software to accurately compute attributes of cell size, morphology, spatial aggregation and color segmentation that signify in situ ecophysiological adaptations in microbial biofilm communities. Computation 3(1):72–98
35. Bölter M, Bloem J, Meiners K, Möller R (2002) Enumeration and biovolume determination of microbial cells-a methodological review and recommendations for applications in ecological research. Biol Fertility of Soils 36(4):249–259
36. Dazzo FB, Klemmer KJ, Chandler R, Yanni YG (2013) In situ ecophysiology of microbial biofilm communities analyzed by CMEIAS computer-assisted microscopy at single-cell resolution. Diversity 5(3):426–460
37. Costa J, Mesquita D, Amaral A, Alves M, Ferreira E (2013) Quantitative image analysis for the characterization of microbial aggregates in biological wastewater treatment: a review. Environ Sci Pollut Res 20(9):5887–5912
38. Li C, Wang K, Xu N (2019) A survey for the applications of content-based microscopic image analysis in microorganism classification domains. Art Intell Rev 51(4):577–646
39. Gmür R, Guggenheim B, Giertsen E, Thurnheer T (2000) Automated immunofluorescence for enumeration of selected taxa in supragingival dental plaque. Eu J Oral Sci 108(5):393–402
40. Li C, Kulwa F, Zhang J, Li Z, Xu H, Zhao X (2020) A review of clustering methods in microorganism image analysis. Informat Technol Biomed 1186:13–25
41. Andreini P, Bonechi S, Bianchini M, Garzelli A, Mecocci A (2016) Automatic image classification for the urinoculture screening. Comput Biol Med 70:12–22
42. Pan Q, Zhang L, Dai G, Zhang H (1999) Two denoising methods by wavelet transform. IEEE Transac Signal Proc 47(12):3401–3406
43. Zhu, S., Xia, X., Zhang, Q., Belloulata, K.: An image segmentation algorithm in image processing based on threshold segmentation. In: 2007 third international IEEE conference on signal-image technologies and internet-based system. pp. 673–678. IEEE (2007)
44. Sekertekin A (2021) A survey on global thresholding methods for mapping open water body using Sentinel-2 satellite imagery and normalized difference water index. Archives Comput Methods Eng 28(3):1335–1347
45. Perez A, Gonzalez RC (1987) An iterative thresholding algorithm for image segmentation. IEEE Transac Pattern Analysis Machine Intell 9(6):742–751
46. Otsu N (1979) A threshold selection method from gray-level histograms. IEEE transactions on systems, man, and cybernetics 9(1):62–66
47. Xu X, Xu S, Jin L, Song E (2011) Characteristic analysis of Otsu threshold and its applications. Pattern Recog Lett 32(7):956–961
48. Haralick RM, Shapiro LG (1985) Image segmentation techniques. Computer Vision, graphics, and image processing 29(1):100–132
49. Gonzales, R.C., Woods, R.E.: Digital image processing (2002)
50. Strahler AN (1957) Quantitative analysis of watershed geomorphology. Eos, Transac Am Geophys Union 38(6):913–920
51. Mukhopadhyay S, Chanda B (2003) Multiscale morphological segmentation of gray-scale images. IEEE Transac Image Proc 12(5):533–549
52. Ziegler U, Groscurth P (2004) Morphological features of cell death. Physiology 19(3):124–128
53. Mariey L, Signolle J, Amiel C, Travert J (2001) Discrimination, classification, identification of microorganisms using FTIR spectroscopy and chemometrics. Vibrational Spectroscopy 26(2):151–159
54. Hay A (1988) The derivation of global estimates from a confusion matrix. Internat J Remote Sens 9(8):1395–1398
55. Buckland M, Gey F (1994) The relationship between recall and precision. J Am Society Informat Sci 45(1):12–19
56. Chicco D, Jurman G (2020) The advantages of the Matthews correlation coefficient (MCC) over F1 score and accuracy in binary classification evaluation. BMC Genomics 21(1):6
57. Zhang, H., Fritts, J.E., Goldman, S.A.: Image segmentation evaluation: A survey of unsupervised methods. computer vision and image understanding **110**(2), 260–280 (2008)
58. Anuar N, Sultan ABM (2010) Validate conference paper using dice coefficient. Comput Informat Sci 3(3):139
59. Rahman, M.A., Wang, Y.: Optimizing intersection-over-union in deep neural networks for image segmentation. In: International symposium on visual computing. pp. 234–244. Springer (2016)
60. Krambeck C, Krambeck HJ, Overbeck J (1981) Microcomputer-assisted biomass determination of plankton bacteria on scanning electron micrographs. Appl Environ Microbiol 42(1):142–149
61. Camp CE, Sublette KL (1992) Control of a Thiobacillus denitrificans bioreactor using machine vision. Biotechnol Bioeng 39(5):529–538
62. Lomander A, Schreuders P, Russek-Cohen E, Ali L (2002) A method for rapid analysis of biofilm morphology and coverage on glass and polished and brushed stainless steel. Transactions of the Asae 45(2):479
63. Petrisor AI, Cuc A, Decho AW (2004) Reconstruction and computation of microscale biovolumes using geographical information systems: potential difficulties. Res Microbiol 155(6):447–454
64. Bjørnsen PK (1986) Automatic determination of bacterioplankton biomass by image analysis. Appl Environ Microbiol 51(6):1199–1204
65. Heydorn A, Nielsen AT, Hentzer M, Sternberg C, Givskov M, Ersbøll BK, Molin S (2000) Quantification of biofilm structures by the novel computer program COMSTAT. Microbiology 146(10):2395–2407
66. Garófano G, Venancio C, Suazo C, Almeida P (2005) Application of the wavelet image analysis technique to monitor cell concentration in bioprocesses. Brazilian J Chem Eng 22(4):573–583
67. Mueller LN, De Brouwer JF, Almeida JS, Stal LJ, Xavier JB (2006) Analysis of a marine phototrophic biofilm by confocal laser scanning microscopy using the new image quantification software PHLIP. BMC Ecol 6(1):1
68. Ross SS, Reinhardt JM, Fiegel J (2012) Enhanced analysis of bacteria susceptibility in connected biofilms. J Microbiol Methods 90(1):9–14
69. Boman C, Jialin Y, Guanxin L, Linyan H, Fang L, Hua Y (2008) Sequential development of biofilm spatial structure of Pseudomonas Aeruginosa tagged with SYTO9/PI. J Third Military Med Univ 30(5):390–392
70. Mesquita D, Dias O, Elias R, Amaral AL, Ferreira E (2010) Dilution and magnification effects on image analysis applications in activated sludge characterization. Micros Microanal 16(05):561–568
71. Bölter M, Möller R, Dzomla W (1993) Determination of bacterial biovolume with epifluorescence microscopy: comparison of

size distributions from image analysis and size classifications. Micron 24(1):31–40
72. Rodríguez SJ, Bishop PL (2007) Three-dimensional quantification of soil biofilms using image analysis. Environ Eng Sci 24(1):96–103
73. Schönholzer F, Hahn D, Zeyer J (1999) Origins and fate of fungi and bacteria in the gut of Lumbricus terrestris L. studied by image analysis. FEMS Microbiol Ecol 28(3):235–248
74. Estep KW, MacIntyre F, Hjorleifsson E, Sieburth J (1986) MacImage: a user-friendly image-analysis system for the accurate mensuration of marine organisms. Mar Ecol Prog Ser 33:243–253
75. Lawrence J, Korber D, Caldwell D (1989) Computer-enhanced darkfield microscopy for the quantitative analysis of bacterial growth and behavior on surfaces. J Microbiol Methods 10(2):123–138
76. Korber DR, Lawrence JR, Sutton B, Caldwell DE (1989) Effect of laminar flow velocity on the kinetics of surface recolonization by Mot+ and Mot- Pseudomonas fluorescens. Microbial Ecol 18(1):1–19
77. An YH, Friedman RJ, Draughn RA, Smith EA, Nicholson JH, John JF (1995) Rapid quantification of staphylococci adhered to titanium surfaces using image analyzed epifluorescence microscopy. J Microbiol Methods 24(1):29–40
78. Tackx M, Zhu L, De Coster W, Billones R, Daro M (1995) Measuring selectivity of feeding by estuarine copepods using image analysis combined with microscopic and Coulter counting. ICES J Marine Sci 52(3–4):419–425
79. Kuehn M, Hausner M, Bungartz HJ, Wagner M, Wilderer PA, Wuertz S (1998) Automated confocal laser scanning microscopy and semiautomated image processing for analysis of biofilms. Appl Environ Microbiol 64(11):4115–4127
80. Gayen K, Venkatesh K (2008) Quantification of cell size distribution as applied to the growth of Corynebacterium glutamicum. Microbiol Res 163(5):586–593
81. de Paz LEC (2009) Image analysis software based on color segmentation for characterization of viability and physiological activity of biofilms. Appl Environ Microbiol 75(6):1734–1739
82. Puyen ZM, Villagrasa E, Maldonado J, Esteve I, Solé A (2012) Viability and biomass of Micrococcus luteus DE2008 at different salinity concentrations determined by specific fluorochromes and CLSM-image analysis. Curr Microbiol 64(1):75–80
83. Ghiţă S., Acomi, N.: Optimizing the heat exchange in ballast water treatment using software monitoring methods. Global Journal on Technology **4**(2) (2013)
84. Folland I, Trione D, Dazzo F (2014) Accuracy of biovolume formulas for cmeias computer-assisted microscopy and body size analysis of morphologically diverse microbial populations and communities. Microbial Ecol 68(3):596–610
85. Dazzo F, Gross C (2013) CMEIAS Quadrat Maker: a digital software tool to optimize grid dimensions and produce quadrat images for landscape ecology spatial analysis. J Ecosystem and Ecography 3(4):136
86. Congestri R, Federici R, Albertano P (2000) Evaluating biomass of Baltic filamentous cyanobacteria by image analysis. Aquatic Microbial Ecol 22(3):283–290
87. Billones R, Tackx M, Flachier A, Zhu L, Daro M (1999) Image analysis as a tool for measuring particulate matter concentrations and gut content, body size, and clearance rates of estuarine copepods: validation and application. J Marine Syst 22(2–3):179–194
88. Shuxin Z, Yun C, Weihua T, Shiru J (2004) Morphological analysis of monascuson surface fermentation. Microbiol China 31(4):65–70
89. Ernst B, Neser S, O'Brien E, Hoeger SJ, Dietrich DR (2006) Determination of the filamentous cyanobacteria Planktothrix rubescens in environmental water samples using an image processing system. Harmful Algae 5(3):281–289
90. Almesjö L, Rolff C (2007) Automated measurements of filamentous cyanobacteria by digital image analysis. Limnol Oceanography: Methods 5(7):217–224
91. Córdoba-Matson MV, Gutiérrez J, Porta-Gándara MÁ (2010) Evaluation of Isochrysis galbana (clone T-ISO) cell numbers by digital image analysis of color intensity. J Appl Phycol 22(4):427–434
92. Jung SK, Lee SB (2003) Image analysis of light distribution in a photobioreactor. Biotechnol Bioeng 84(3):394–397
93. Álvarez E, Lopez-Urrutia A, Nogueira E (2012) Improvement of plankton biovolume estimates derived from image-based automatic sampling devices: application to FlowCAM. J Plankton Res 34(6):454–469
94. Gandola E, Antonioli M, Traficante A, Franceschini S, Scardi M, Congestri R (2016) ACQUA: Automated cyanobacterial quantification algorithm for toxic filamentous genera using spline curves, pattern recognition and machine learning. J Microbiol Methods 124:48–56
95. Akiba T, Kakui Y (2000) Design and testing of an underwater microscope and image processing system for the study of zooplankton distribution. IEEE J Oceanic Eng 25(1):97–104
96. Lecault V, Patel N, Thibault J (2009) An image analysis technique to estimate the cell density and biomass concentration of Trichoderma reesei. Lett Appl Microbiol 48(4):402–407
97. Albertano P (2002) Image analysis for qualitative and quantitative evaluation of planktic cyanobacteria. RAPPORTI ISTISAN 2(9):64–69
98. Leal C, Amaral AL, de Lourdes Costa M (2016) Microbial-based evaluation of foaming events in full-scale wastewater treatment plants by microscopy survey and quantitative image analysis. Environ Sci Pollut Res 23(15):15638–15650
99. Alcaraz M, Saiz E, Calbet A, Trepat I, Broglio E (2003) Estimating zooplankton biomass through image analysis. Marine Biol 143(2):307–315
100. Miszkiewicz, H., Bizukojc, M., Rozwandowicz, A., Bielecki, S.: Physiological properties and enzymatic activities of Rhizopus oligosporus in solid state fermentations. Electronic Journal of Polish Agricultural Universities **7** (2004)
101. Couri S, Merces E, Neves B, Senna L (2006) Digital image processing as a tool to monitor biomass growth in Aspergillus niger 3T5B8 solid-state fermentation: preliminary results. J Micros 224(3):290–297
102. Dutra, J.C., da Terzi, S.C., Bevilaqua, J.V., Damaso, M.C., Couri, S., Langone, M.A., Senna, L.F.: Lipase production in solid-state fermentation monitoring biomass growth of Aspergillus niger using digital image processing. In: Biotechnology for Fuels and Chemicals, pp. 431–443. Springer (2007)
103. Solé A, Mas J, Esteve I (2007) A new method based on image analysis for determining cyanobacterial biomass by CLSM in stratified benthic sediments. Ultramicroscopy 107(8):669–673
104. Barry DJ, Chan C, Williams GA (2009) Morphological quantification of filamentous fungal development using membrane immobilization and automatic image analysis. J Indus Microbiol Biotechnol 36(6):787
105. Solé A, Diestra E, Esteve I (2009) Confocal laser scanning microscopy image analysis for cyanobacterial biomass determined at microscale level in different microbial mats. Microbial Ecol 57(4):649–656
106. Posch T, Franzoi J, Prader M, Salcher MM (2009) New image analysis tool to study biomass and morphotypes of three major bacterioplankton groups in an alpine lake. Aquatic Microbial Ecol 54(2):113–126

107. Alum A, Mobasher B, Rashid A, Abbaszadegan M (2009) Image analyses-based nondisruptive method to quantify algal growth on concrete surfaces. J Environ Eng 135(3):185–190
108. Song S, Yongkun B, Xiaoxia S (2013) Relationship between shape parameters and dry weight of the dominant zooplankton in Jiaozhou bay based on image method. Oceanologia et Limnologia Sinica 44(1):15–22
109. Mohan J, Saros J, Stone JR (2021) On the matter of phytoplankton: a novel method using 3D computer models to calculate biovolume of microorganisms. Limnol Oceanography: Methods 19(5):331–339
110. Mcnair H, Hammond CN, Menden-Deuer S (2021) Phytoplankton carbon and nitrogen biomass estimates are robust to volume measurement method and growth environment. J Plankton Res 43(2):103–112
111. Borics G, Lerf V, Enikő T, Stanković I, Pickó L, Béres V, Várbíró G et al (2021) Biovolume and surface area calculations for microalgae, using realistic 3D models. Sci Total Environ 773:145538
112. Awadh AA, Kelly AF, Forster-Wilkins G, Wertheim D, Giddens R, Gould SW, Fielder MD (2021) Visualisation and biovolume quantification in the characterisation of biofilm formation in Mycoplasma fermentans. Sci Rep 11(1):1–9
113. Eniko, T., Lerf, V., Toth, I., Kisantal, T., Varbiro, G., Vasas, G., Viktoria, B., Gorgenyi, J., Lukacs, A., Kokai, Z., et al.: Uncertainties of cell number estimation in cyanobacterial colonies and the potential use of sphere packing. bioRxiv (2022)
114. Zhao, P., Li, C., Rahaman, M.M., Xu, H., Ma, P., Yang, H., Sun, H., Jiang, T., Xu, N., Grzegorzek, M.: EMDS-6: Environmental Microorganism Image Dataset Sixth Version for Image Denoising, Segmentation, Feature Extraction, Classification, and Detection Method Evaluation. Frontiers in Microbiology p. 1334 (2022)
115. Dietler N, Minder M, Gligorovski V, Economou AM, Joly DAHL, Sadeghi A, Chan CHM, Koziński M, Weigert M, Bitbol AF et al (2020) A convolutional neural network segments yeast microscopy images with high accuracy. Nat Commun 11(1):1–8
116. Fan L, Zhang F, Fan H, Zhang C (2019) Brief review of image denoising techniques. Visual Computing for Industry, Biomedicine, and Art 2(1):1–12
117. Barbedo JGA (2013) An algorithm for counting microorganisms in digital images. IEEE Latin America Transac 11(6):1353–1358
118. Zhang, J., Li, C., Kosov, S., Grzegorzek, M., Shirahama, K., Jiang, T., Sun, C., Li, Z., Li, H.: LCU-Net: A Novel Low-cost U-Net for Environmental Microorganism Image Segmentation. Pattern Recognition p. 107885 (2021)
119. Rani, P., Kotwal, S., Manhas, J., Sharma, V., Sharma, S.: Machine learning and deep learning based computational approaches in automatic microorganisms image recognition: methodologies, challenges, and developments. Archives of Computational Methods in Engineering pp. 1–37 (2021)
120. Garcia-Garcia, A., Orts-Escolano, S., Oprea, S., Villena-Martinez, V., Garcia-Rodriguez, J.: A review on deep learning techniques applied to semantic segmentation. arXiv preprint arXiv:1704.06857 (2017)
121. Huttenlocher DP, Klanderman GA, Rucklidge WJ (1993) Comparing images using the Hausdorff distance. IEEE Transact Pattern Anal Machine Intel 15(9):850–863
122. Kosov S, Shirahama K, Li C, Grzegorzek M (2018) Environmental microorganism classification using conditional random fields and deep convolutional neural networks. Pattern Recog 77:248–261
123. Zhao, P., Li, C., Rahaman, M., Xu, H., Yang, H., Sun, H., Jiang, T., Grzegorzek, M.: A Comparative Study of Deep Learning Classification Methods on a Small Environmental Microorganism Image Dataset (EMDS-6): From Convolutional Neural Networks to Visual Transformers. Frontiers in Microbiology **13** (2022)
124. Kulwa, F., Li, C., Zhang, J., Shirahama, K., Kosov, S., Zhao, X., Sun, H., Jiang, T., Grzegorzek, M.: A New Pairwise Deep Learning Feature For Environmental Microorganism Image Analysis. arXiv preprint arXiv:2102.12147 (2021)
125. Li C, Shirahama K, Grzegorzek M (2016) Environmental microbiology aided by content-based image analysis. Pattern Anal Appl 19(2):531–547
126. Su, M.C., Cheng, C.Y., Wang, P.C.: A neural-network-based approach to white blood cell classification. The scientific world journal **2014** (2014)
127. Li C, Shirahama K, Grzegorzek M (2015) Application of content-based image analysis to environmental microorganism classification. Biocybernetics Biomed Eng 35(1):10–21
128. Xu H, Li C, Rahaman MM, Yao Y, Li Z, Zhang J, Kulwa F, Zhao X, Qi S, Teng Y (2020) An enhanced framework of generative adversarial networks (EF-GANs) for environmental microorganism image augmentation with limited rotation-invariant training data. IEEE Access 8:187455–187469
129. Li, C., Ma, P., Rahaman, M.M., Yao, Y., Zhang, J., Zou, S., Zhao, X., Grzegorzek, M.: A State-of-the-art Survey of Object Detection Techniques in Microorganism Image Analysis: from Traditional Image Processing and Classical Machine Learning to Current Deep Convolutional Neural Networks and Potential Visual Transformers. arXiv preprint arXiv:2105.03148 (2021)
130. Rahaman MM, Li C, Yao Y, Kulwa F, Wu X, Li X, Wang Q (2021) DeepCervix: a deep learning-based framework for the classification of cervical cells using hybrid deep feature fusion techniques. Comput Biol Med 136:104649
131. Rahaman MM, Li C, Wu X, Yao Y, Hu Z, Jiang T, Li X, Qi S (2020) A survey for cervical cytopathology image analysis using deep learning. IEEE Access 8:61687–61710
132. Zou, S., Li, C., Sun, H., Xu, P., Zhang, J., Ma, P., Yao, Y., Huang, X., Grzegorzek, M.: TOD-CNN: An effective convolutional neural network for tiny object detection in sperm videos. Computers in Biology and Medicine p. 105543 (2022)
133. Chen, A., Li, C., Zou, S., Rahaman, M.M., Yao, Y., Chen, H., Yang, H., Zhao, P., Hu, W., Liu, W., et al.: SVIA dataset: A new dataset of microscopic videos and images for computer-aided sperm analysis. Biocybernetics and Biomedical Engineering (2022)
134. Li F, Shirahama K, Nisar MA, Köping L, Grzegorzek M (2018) Comparison of feature learning methods for human activity recognition using wearable sensors. Sensors 18(2):679
135. Shirahama K, Grzegorzek M (2016) Towards large-scale multimedia retrieval enriched by knowledge about human interpretation. Multimedia Tools Appl 75(1):297–331
136. Huang X, Shirahama K, Li F, Grzegorzek M (2020) Sleep stage classification for child patients using DeConvolutional Neural Network. Artificial Intel Med 110:101981
137. Huang, X., Li, C., Shen, M., Shirahama, K., Nyffeler, J., Leist, M., Grzegorzek, M., Deussen, O.: Stem cell microscopic image segmentation using supervised normalized cuts. In: 2016 IEEE International Conference on Image Processing (ICIP). pp. 4140–4144. IEEE (2016)
138. Thyagharajan, K., Kalaiarasi, G.: A review on near-duplicate detection of images using computer vision techniques. Archives of Computational Methods in Engineering pp. 1–20 (2020)
139. Qi, Y., Yang, Z., Sun, W., Lou, M., Lian, J., Zhao, W., Deng, X., Ma, Y.: A Comprehensive Overview of Image Enhancement Techniques. Archives of Computational Methods in Engineering pp. 1–25 (2021)

140. Chen X, Zhou X, Wong ST (2006) Automated segmentation, classification, and tracking of cancer cell nuclei in time-lapse microscopy. IEEE Transact Biomed Eng 53(4):762–766
141. Kulwa F, Li C, Zhao X, Cai B, Xu N, Qi S, Chen S, Teng Y (2019) A state-of-the-art survey for microorganism image segmentation methods and future potential. IEEE Access 7:100243–100269
142. Zhang, J., Xu, N., Li, C., Rahaman, M.M., Yao, Y.D., Lin, Y.H., Zhang, J., Jiang, T., Qin, W., Grzegorzek, M.: An application of Pixel Interval Down-sampling (PID) for dense tiny microorganism counting on environmental microorganism images. arXiv preprint arXiv:2204.01341 (2022)
143. Amaral A, Ferreira E (2005) Activated sludge monitoring of a wastewater treatment plant using image analysis and partial least squares regression. Analytica Chimica Acta 544(1–2):246–253
144. Cross H, Gilliland D, Durland P, Seideman S (1983) Beef carcass evaluation by use of a video image analysis system. J Animal Sci 57(4):908–917
145. Pettipher G, Rodrigues UM (1982) Semi-automated counting of bacteria and somatic cells in milk using epifluorescence microscopy and television image analysis. J Appl Bacteriol 53(3):323–329
146. Yu H, MacGregor JF (2004) Monitoring flames in an industrial boiler using multivariate image analysis. AIChE J 50(7):1474–1483
147. Bharati M, MacGregor J, Tropper W (2003) Softwood lumber grading through on-line multivariate image analysis techniques. Industrial & Eng Chem Res 42(21):5345–5353
148. Yang, Y., Li, G., Wu, Z., Su, L., Huang, Q., Sebe, N.: Reverse perspective network for perspective-aware object counting. In: Proceedings of the IEEE/CVF Conference on Computer Vision and Pattern Recognition. pp. 4374–4383 (2020)
149. Jiang, X., Xiao, Z., Zhang, B., Zhen, X., Cao, X., Doermann, D., Shao, L.: Crowd counting and density estimation by trellis encoder-decoder networks. In: Proceedings of the IEEE/CVF Conference on Computer Vision and Pattern Recognition. pp. 6133–6142 (2019)
150. Cholakkal H, Sun G, Khan FS, Shao L (2019) Object counting and instance segmentation with image-level supervision. In: Proceedings of the IEEE/CVF Conference on Computer Vision and Pattern Recognition. pp. 12397–12405
151. Jaderberg, M., Simonyan, K., Zisserman, A., Kavukcuoglu, K.: Spatial transformer networks. arXiv preprint arXiv:1506.02025 (2015)
152. Hu, J., Shen, L., Sun, G.: Squeeze-and-excitation networks. In: Proceedings of the IEEE conference on computer vision and pattern recognition. pp. 7132–7141 (2018)
153. Han, K., Wang, Y., Chen, H., Chen, X., Guo, J., Liu, Z., Tang, Y., Xiao, A., Xu, C., Xu, Y., et al.: A Survey on Visual Transformer. arXiv preprint arXiv:2012.12556 (2020)
154. Dosovitskiy, A., Beyer, L., Kolesnikov, A., Weissenborn, D., Zhai, X., Unterthiner, T., Dehghani, M., Minderer, M., Heigold, G., Gelly, S., et al.: An image is worth 16x16 words: Transformers for image recognition at scale. arXiv preprint arXiv:2010.11929 (2020)
155. Lee CW, Ren YJ, Marella M, Wang M, Hartke J, Couto SS (2020) Multiplex immunofluorescence staining and image analysis assay for diffuse large B cell lymphoma. J Immunol Meth 478:112714
156. Bloem J, Veninga M, Shepherd J (1995) Fully automatic determination of soil bacterium numbers, cell volumes, and frequencies of dividing cells by confocal laser scanning microscopy and image analysis. Appl Environ Microbiol 61(3):926–936
157. Pernthaler J, Pernthaler A, Amann R (2003) Automated enumeration of groups of marine picoplankton after fluorescence in situ hybridization. Appl Environ Microbiol 69(5):2631–2637

Publisher's Note Springer Nature remains neutral with regard to jurisdictional claims in published maps and institutional affiliations.

Springer Nature or its licensor holds exclusive rights to this article under a publishing agreement with the author(s) or other rightsholder(s); author self-archiving of the accepted manuscript version of this article is solely governed by the terms of such publishing agreement and applicable law.